



1 **Coupled eco-hydrology and biogeochemistry algorithms enable simulation of water table**
2 **depth effects on boreal peatland net CO₂ exchange**

3

4 Mohammad Mezbahuddin*^{1,2}, Robert F. Grant², and Lawrence B. Flanagan³

5

6 ¹*Environmental Stewardship Branch, Alberta Agriculture and Forestry, Edmonton, AB, Canada*

7 ²*Department of Renewable Resources, University of Alberta, Edmonton, AB, Canada*

8 ³*Department of Biological Sciences, University of Lethbridge, AB, Canada*

9

10 *corresponding author. Email addresses: symon.mezbahuddin@gov.ab.ca,

11 mezbahud@ualberta.ca.



12 Abstract

13 Water table depth (WTD) effects on net ecosystem CO₂ exchange of boreal peatlands are
14 largely mediated by hydrological effects on peat biogeochemistry, and eco-physiology of
15 peatland vegetation. Lack of representation of these effects in carbon models currently limits our
16 predictive capacity for changes in boreal peatland carbon deposits under future drier and warmer
17 climates. We therefore tested whether the effects of WTD variation on net ecosystem CO₂
18 exchange of a Western Canadian boreal fen peatland could be modelled through a process-level
19 coupling of a prognostic WTD dynamic, which arises from equilibrium between vertical and
20 lateral water fluxes, with oxygen transport, which controls energy yields from microbial and root
21 oxidation-reduction reactions, and vascular and non-vascular plant water relations in an
22 ecosystem model *ecosys*. *Ecosys* successfully simulated a May-October WTD drawdown by
23 ~0.25 m measured in the fen from 2004 to 2008, which was attributed to reduced precipitation
24 relative to evapotranspiration, and reduced lateral recharge relative to discharge. This WTD
25 drawdown hastened oxygen transport to microbial and root surfaces, enabling greater microbial
26 and root energy yields, and peat and litter decomposition, which raised modelled ecosystem
27 respiration (R_e) by ~0.26 $\mu\text{mol CO}_2 \text{ m}^{-2} \text{ s}^{-1}$ per 0.1 m of WTD drawdown. It also augmented
28 nutrient mineralization, and hence root nutrient availability and uptake, which resulted in
29 improved leaf nutrient (nitrogen) status that facilitated carboxylation, and raised modelled
30 vascular gross primary productivity (GPP) and plant growth. The increase in modelled vascular
31 GPP exceeded declines in modelled non-vascular (moss) GPP due to greater shading from
32 increased vascular plant growth, and moss drying from near surface peat desiccation, thereby
33 causing a net increase in modelled growing season GPP by ~0.39 $\mu\text{mol CO}_2 \text{ m}^{-2} \text{ s}^{-1}$ per 0.1 m of
34 WTD drawdown. Similar increases in GPP and R_e left no significant WTD effects on modelled



35 seasonal and interannual variations in net ecosystem productivity (NEP). These modelled trends
36 were corroborated against eddy covariance hourly net CO₂ fluxes (modelled vs. measured:
37 $R^2 \sim 0.8$, slopes $\sim 1 \pm 0.1$, intercepts $\sim 0.05 \mu\text{mol m}^{-2} \text{s}^{-1}$), and against other automated chamber,
38 biometric, and laboratory measurements. Modelled drainage as an analog for climate change
39 showed that this boreal peatland would switch from a large carbon sink (NEP $\sim 160 \text{ g C m}^{-2} \text{ yr}^{-1}$)
40 to carbon neutrality (NEP $\sim 10 \text{ g C m}^{-2} \text{ yr}^{-1}$) should water table deepened by a further $\sim 0.5 \text{ m}$.
41 Therefore, representing the effects of interactions among hydrology, biogeochemistry and plant
42 physiological ecology on ecosystem carbon, water, and nutrient cycling in global carbon models
43 would improve our predictive capacity for changes in boreal peatland carbon sequestration under
44 changing climates.



45 1. Introduction

46 Northern boreal peatlands have been accumulating carbon (C) at a rate of about 20-30 g
47 yr⁻¹ over several thousand years (Gorham, 1991; Turunen et al., 2002). Drier and warmer future
48 climates can affect the resilience of long-term boreal peatland C stocks by lowering water table
49 (WT) that can halt or even reverse the C accumulation in boreal peatlands (Limpens et al., 2008;
50 Dise, 2009; Frohling et al., 2011). To maintain and protect the C sequestration potentials of
51 boreal peatlands we need an improved predictive capacity of how these C stocks would behave
52 under future drier and warmer climates. Despite the need, boreal peatland C processes are
53 currently under-represented in global C models largely due to inadequate simulation of
54 hydrologic feedbacks to C cycles (St-Hilaire et al., 2010; Sulman et al., 2012). This shortfall can
55 be overcome by integrating interactions between eco-hydrology of peatland vegetation, and peat
56 biogeochemistry into finer resolution process models that can eventually be scaled up into larger
57 spatial and temporal scale C models (Waddington et al., 2015).

58 The hydrologic feedbacks to boreal peatland C processes are largely mediated by water
59 table depth (WTD) variation and its effects on peat-microbe-plant-atmosphere exchanges of C,
60 energy, water and nutrients (Grant et al., 2012). WTD drawdown can affect net ecosystem
61 productivity (NEP) of boreal peatlands through its effects on ecosystem respiration (R_e) and
62 gross primary productivity (GPP). Receding WT can cause peat pore drainage that enhances
63 microbial O₂ availability, energy yields, growth and decomposition and hence increases R_e
64 (Sulman et al., 2009, 2010; Cai et al., 2010; Flanagan and Syed, 2011; Peichl et al., 2014). The
65 rate of increase in R_e due to the WTD drawdown may vary with peat moisture retention and
66 quality of peat forming substrates (Preston et al., 2012). For instance, peats with low moisture
67 retention exhibit more rapid pore drainage than those with high moisture retention thus causing



68 more increase in R_e for similar WTD drawdowns (Parmentier et al., 2009; Sulman et al., 2009,
69 2010; Cai et al., 2010). Peats formed from *Sphagnum* mosses degrade at rates slower than those
70 formed from remains of vascular plants (Moore and Basiliko, 2006). So for similar WTD
71 drawdowns, moss peats would generate less increase in microbial decomposition and hence R_e
72 than would sedge, reed or woody peats (Updegraff et al., 1995). Continued WTD drawdown can
73 also cause near surface peat desiccation from inadequate recharge through capillary rise from
74 deeper WT. Desiccation of near surface or shallow peat layers can cause a reduction in microbial
75 decomposition that can partially or fully offset the increased decomposition in the deeper peat
76 layers thereby yielding indistinct net effects of WTD drawdown on R_e (Dimitrov et al., 2010a).

77 The interactions between WTD and GPP vary across peatlands depending upon peat
78 forming vegetation. For instance, increased aeration due to WTD drawdown enhances root O_2
79 availability and growth in vascular plants (Lieffers and Rothwell, 1987; Murphy et al., 2009).
80 Enhanced root growth is also associated with greater root nutrient availability and uptake from
81 more rapid mineralization facilitated by greater microbial energy yields, growth and
82 decomposition under deeper WT (Choi et al., 2007). Greater root nutrient uptake in turns
83 increases the rate of vascular CO_2 fixation and hence GPP (Sulman et al., 2009, 2010; Cai et al.,
84 2010; Flanagan and Syed, 2011; Peichl et al., 2014). WTD drawdown, however, does not affect
85 the non-vascular (e.g., moss) GPP in the same way it does the vascular GPP (Lafleur et al.,
86 2005). Non-vascular plants mostly depend upon the water available for uptake in the near surface
87 or shallow peat layers (Dimitrov et al., 2011). These layers can drain quickly with receding WT
88 and thus have to depend on moisture supply through capillary rise from deeper WT (Dimitrov et
89 al., 2011; Peichl et al., 2014). If recharge through the capillary rise is not adequate, near surface
90 peat desiccation occurs which slows moss water uptake, causes eventual drying of mosses and



91 reduces moss GPP (Lafleur et al., 2005; Riutta 2008; Sonnentag et al., 2010; Sulman et al., 2010;
92 Dimitrov et al., 2011; Kuiper et al., 2014; Peichl et al., 2014). Near surface peat desiccation also
93 suppresses vascular root water uptake from the desiccated layers (Lafleur et al., 2005; Dimitrov
94 et al., 2011). But enhanced root growth and elongation facilitated by improved O₂ status in the
95 newly aerated deeper peat layers under deeper WT enables vascular roots to take up water from
96 wetter deeper layers (Dimitrov et al., 2011). If deeper root water uptake offsets the reduction in
97 water uptake from desiccated near surface layers, vascular transpiration (T), canopy stomatal
98 conductance (g_c) and hence GPP are sustained under deeper WT (Dimitrov et al., 2011). But if
99 the WT falls below certain threshold level under which deeper root water uptake can no longer
100 sustain vascular T , g_c and hence vascular GPP declines (Lafleur et al., 2005; Wu et al., 2010).

101 Therefore, WTD variation can affect boreal peatland NEP through its effects on peat
102 moisture and aeration and consequent root and microbial oxidation-reduction reactions and
103 energy yields. So, to adequately predict how boreal peatlands would behave under future drier
104 and warmer climates, a peatland C model needs to have sufficient representation of WTD
105 dynamics that determine the boundary between aerobic and anaerobic zones and controls peat
106 biogeochemistry. However, most of the current process-based peatland C models either do not
107 have a prognostic WTD dynamic that prevent simulation of a continuous anaerobic zone below
108 WT (e.g., Baker et al., 2008; Schaefer et al., 2008; Tian et al., 2010), or do not simulate peat
109 saturation since any water in excess of field capacity is drained in those models (e.g., Gerten et
110 al., 2004; Krinner et al., 2005; Weng and Luo, 2008). Moreover, instead of explicitly simulating
111 the above-described hydrological and biological interactions between peat aeration and
112 biogeochemistry, most of those models use scalar functions of soil moisture contents to inhibit R_e
113 and GPP under low or high moisture conditions (e.g., Frohling et al., 2002; Zhang et al., 2002;



114 Bond-Lamberty et al., 2007; St-Hilaire et al., 2010; Sulman et al., 2012). Consequently, those
115 peatland C models could not simulate declines in GPP and R_e due to shallow WT while
116 simulating WTD effects on CO₂ exchange of peatlands across northern US and Canada (Sulman
117 et al., 2012). Furthermore, the approach of using scalar functions to simulate moisture limitations
118 to GPP and R_e requires site-specific parameterization of the scalar functions which makes this
119 approach less suitable when scaling up across different peatlands.

120 **1.1. Objective and rationale**

121 To overcome the inadequacies in peatland C models as discussed above, we represented a
122 prognostic and dynamic WTD, and a soil moisture retention scheme that are coupled with
123 microbial and root oxidation-reduction reactions, energy yields, growth, and uptake within a soil-
124 plant-microbe-atmosphere water, C and nutrient (nitrogen, phosphorus) scheme in a terrestrial
125 process model *ecosys*. Our objective was to test whether this coupling of hydrology with
126 biogeochemistry and plant physiological ecology in *ecosys* would enable successful simulation
127 of diurnal, seasonal and interannual variations in net CO₂ exchange as affected by variations in
128 WTD over a drying period from 2004 to 2009 in a western Canadian boreal fen peatland in
129 Alberta, Canada (will be termed as WPL hereafter) (Syed et al., 2006; Flanagan and Syed, 2011).
130 For this purpose, *ecosys* algorithms would first be fed by inputs for peat hydrological, biological,
131 chemical and physical properties, and plant physiology measured at the WPL or similar
132 peatlands. Then the modelled outputs for net ecosystem CO₂ exchange and WTD would be
133 tested against site measurements at the WPL. The tested modelled outputs would further be
134 examined to explain WTD effects on C processes at this northern boreal fen.

135 In the past, similar coupling of hydrological, biological and ecological feedbacks enabled
136 *ecosys* to successfully simulate WTD effects on net ecosystem CO₂ exchange of two contrasting



137 bog peatlands e.g., (1) a northern shrub-moss peat bog at Mer Bleue, Ontario, Canada (Dimitrov
138 et al., 2011), and (2) a tropical woody peat bog at Palangkaraya, Central Kalimantan, Indonesia
139 (Mezbahuddin et al., 2014); and a northern shrub-sedge fen peatland at Lost Creek, Wisconsin,
140 USA (Grant et al., 2012). But the mixture of moss and woody peats in the boreal fen peatland
141 under current study had a moisture retention characteristic that differed significantly from all the
142 peatlands in those previous studies (Mezbahuddin et al., 2016). Peats in those previous studies
143 drained as soon as the matric water potential (ψ_m) fell below zero. On the contrary, peats under
144 current study held moisture content close to saturation and did not drain until ψ_m fell below ~-
145 0.004 MPa (Mezbahuddin et al., 2016). Consequently, the Campbell type (Campbell, 1974)
146 power function in *ecosys*, that was used to simulate peat moisture retention scheme in those
147 previous simulations, significantly underestimated peat moisture content in this boreal fen
148 (Mezbahuddin et al., 2016). However, substitution of the existing power function in *ecosys* with
149 a sigmoidal logistic function (van Genuchten, 1980) significantly improved simulation of peat
150 moisture retention over a wide range of moisture conditions in this boreal fen peatland
151 (Mezbahuddin et al., 2016). Since peat moisture retention largely mediates peat oxygenation and
152 hence peatland biogeochemistry, plant water relations, and CO₂ fixation, testing of *ecosys*
153 algorithms with the inclusion of the improved moisture retention scheme against the
154 measurements at the WPL would offer a further test of robustness of process level modelling of
155 hydrological feedbacks to peatland CO₂ exchange. Moreover, WPL differed from those other
156 peatlands, where *ecosys* algorithms of eco-hydrological and biogeochemical feedbacks were
157 previously tested, either in climate (e.g., boreal vs. temperate vs. tropical), or hydrology (e.g., fen
158 vs. bog), or peatland vegetation (e.g., non-vascular vs. vascular), or peat forming substrates (e.g.,
159 moss vs. sedge vs. woody peats), or depth of peat deposits, or in any combination of these



160 peatland characteristics (Dimitrov et al., 2011; Grant et al., 2012; Mezbahuddin et al., 2014,
161 2015, 2016). Since these peatland characteristics predominantly govern hydrological regulations
162 to peatland C processes, further testing of *ecosys* algorithms at the WPL would thus test the
163 versatility and robustness of coupled ecology, hydrology and biogeochemistry algorithms in
164 simulating and explaining WTD effects on net ecosystem CO₂ exchange across contrasting
165 peatlands. Moreover, since hydrological feedbacks to key peatland C processes are highly non-
166 linear and site-specific, testing of *ecosys* algorithms across contrasting peatlands would also
167 facilitate formation of a modelling platform for scaling up simulations of those feedbacks across
168 peatlands at larger spatial scales i.e., national, regional, continental or global as also
169 recommended by Waddington et al. (2015).

170 1.2. Hypotheses

171 In a field study using eddy covariance (EC) micro-meteorological approach, Flanagan
172 and Syed (2011) found no net effect of WTD drawdown from 2004-2009 caused by
173 progressively drier and warmer weather on NEP of WPL. From the regressions of EC-derived
174 GPP and R_e on site measured WTD, they inferred that the absence of a net effect on NEP was
175 caused by similar increases in GPP and R_e with WTD drawdown. We hypothesize that a
176 prognostic, dynamic WTD driven by equilibrium between vertical and lateral water fluxes that
177 determines root and microbial redox reactions and energy yields, microbial decomposition, root
178 and microbial growth and uptake in *ecosys* would be able to simulate these effects of WTD
179 drawdown on GPP and R_e and hence NEP at the WPL. For this purpose, we tested the following
180 four modelling hypotheses while simulating WTD effects on R_e and GPP of WPL:



181 (1) WTD drawdown would cause peat pore drainage and improve peat aeration that would
182 increase the energy yields from aerobic microbial decomposition and hence would increase R_e in
183 the modelled WPL ecosystem.

184 (2) Enhanced microbial activity due to WTD drawdown would also cause more rapid nutrient
185 mineralization and consequent greater root nutrient availability and uptake, greater leaf nutrient
186 concentrations and hence increased GPP.

187 (3) But when the WT falls below a certain threshold level, inadequate recharge of the near
188 surface peat layers through capillary rise would cause desiccation of those layers. Drying of near
189 surface peat layers and the surface residue can reduce near surface and surface peat respiration
190 that can partially offset the increase in deeper peat respiration due to aeration in hypothesis 1.

191 (4) Near surface peat desiccation would also reduce peat water potential and hydraulic
192 conductivity and hence vascular and non-vascular water uptake from desiccated near surface
193 layers. Since non-vascular mosses depend mainly on near surface peat layers for moisture
194 supply, reduction in moss water uptake would cause a reduction in moss water potential and
195 hence moss GPP. On the contrary, suppression of vascular root water uptake from desiccated
196 near surface layers under deeper WT would be offset by increased deeper root water uptake from
197 newly aerated deeper peat layers with higher water potentials that would sustain vascular canopy
198 water potential (ψ_c), canopy stomatal conductance (g_c) and GPP.

199 **2. Methods**

200 **2.1. Model development**

201 *Ecosys* is a process-based terrestrial ecosystem model that simulates 3D water, energy,
202 carbon and nutrient (nitrogen, phosphorus) cycles in different peatlands (Dimitrov et al., 2011;



203 Grant et al., 2012; Sulman et al., 2012; Mezbahuddin et al., 2014, 2015, 2016). *Ecosys*
204 algorithms that govern the effects of WTD variations on ecosystem net CO₂ exchange which are
205 related to our hypotheses are described below. The equations that are cited within the text are
206 listed in the sections S1-S4 in the supplementary material for further clarification.

207 **2.1.1. Water table depth (WTD)**

208 The WTD in *ecosys* is calculated at the end of each time step as the depth to the top of the
209 saturated zone below which air-filled porosity is zero (Eq. D32). It is the depth at which lateral
210 water flux is in equilibrium with the difference between vertical influxes (precipitation) and
211 effluxes (evapotranspiration). Lateral water transfer between modelled grid cells in *ecosys* and
212 the adjacent ecosystem occurs to and from a set external WTD (WTD_x) over a set distance (L_i)
213 (Fig. 1). The WTD_x represents average watershed WTD with reference to average hummock
214 surface. The WTD in *ecosys* is thus not prescribed, but rather controls, and is controlled by
215 lateral and vertical surface and subsurface water fluxes (Eqs. D1-D31). More detail about how
216 peatland WTD, vertical and lateral soil water flow, and soil moisture retention are modelled in
217 *ecosys* can be found in Dimitrov et al. (2010b) and Mezbahuddin et al. (2015, 2016).

218 **2.1.2. Heterotrophic respiration and WTD**

219 WTD fluctuation in *ecosys*, which arises from variations in the balance between vertical
220 and lateral fluxes, determines the boundary between and the extent of aerobic vs. anaerobic soil
221 zones. So WTD fluctuation affects *ecosys*'s algorithms of organic oxidation-reduction
222 transformations and microbial energy yields, which drive microbial growth, substrate
223 decomposition and uptake (Eqs. A1-A30). Organic transformations in *ecosys* occur in a residue
224 layer and in each of the user defined soil layers within five organic matter-microbe complexes
225 i.e., coarse woody litter, fine non-woody litter, animal manure, particulate organic C and humus.



226 Each of the complexes has three decomposition substrates i.e., solid organic C, sorbed organic C
227 and microbial residue C; the decomposition agent i.e., microbial biomass; and the decomposition
228 product i.e., dissolved organic C (DOC). Rates of the decomposition and resulting DOC
229 production in each of the complexes is a first-order function of the fraction of substrate colonized
230 by active biomasses (M) of diverse microbial functional types (MFTs). The MFTs in *ecosys* are
231 obligate aerobes (bacteria and fungi), facultative anaerobes (denitrifiers), obligate anaerobes
232 (fermenters), heterotrophic (acetotrophic) and autotrophic (hydrogenotrophic) methanogens, and
233 aerobic and anaerobic heterotrophic diazotrophs (non-symbiotic N_2 fixers) (Eqs. A1-A2, A4).
234 Biomass (M) growth of each of the MFTs (Eq. A25a) is calculated from its DOC uptake (Eq.
235 A21). The rate of M growth is driven by energy yield from growth respiration (R_g) (Eq. A20) that
236 is calculated by subtracting maintenance respiration (R_m) (Eq. A18) from heterotrophic
237 respiration (R_h) (Eq. A11). The values of R_h are driven by oxidation of DOC (Eq. A13). DOC
238 oxidation may be limited by microbial O_2 reduction (Eq. A14) driven by microbial O_2 demand
239 (Eq. A16) and constrained by O_2 diffusion calculated from aqueous O_2 concentrations in soil
240 ($[O_{2s}]$) (Eq. A17). Values of $[O_{2s}]$ are maintained by convective-dispersive transport of O_2 from
241 the atmosphere to gaseous and aqueous phases of the soil surface layer (Eq. D41), by convective-
242 dispersive transport of O_2 through gaseous and aqueous phases in adjacent soil layers (Eqs. D42,
243 D44), and by dissolution of O_2 from gaseous to aqueous phases within each soil layer (Eq. D39).
244 Shallow WTD in *ecosys* can cause lower air-filled porosity (θ_g) in the wetter peat layers
245 above the WT. Lower θ_g reduces O_2 diffusivity in the gaseous phase (D_g) (Eq. D44) and gaseous
246 O_2 transport (Eqs. D41-D42) in these layers. Peat layers below the WT have zero θ_g that prevents
247 gaseous O_2 transport in these layers. So, under shallow WT, $[O_{2s}]$ relies more on O_2 transport
248 through the slower aqueous phase (Eq. D42) which causes a decline in $[O_{2s}]$. Decline in $[O_{2s}]$



249 slows O_2 uptake (Eq. A17) and hence R_h (Eq. A14), R_g (Eq. A20) and growth of M (Eq. A25).
 250 Lower M slows decomposition of organic C (Eqs. A1-A2) and production of DOC which further
 251 slows R_h (Eq. A13), R_g and growth of M . Although some MFTs can sustain DOC oxidation by
 252 reducing alternative electron acceptors (e.g., methanogens reducing acetate or CO_2 to CH_4 , and
 253 denitrifiers reducing NO_x to N_2O or N_2), lower energy yields from these reactions reduce R_g (Eq.
 254 A21), and hence M growth, organic C decomposition and subsequent DOC production. Slower
 255 decomposition of organic C under low $[O_{2s}]$ also causes slower decomposition of organic
 256 nitrogen (N) and phosphorus (P) (Eq. A7) and production of dissolved organic nitrogen (DON)
 257 and phosphorus (DOP), which causes slower uptake of microbial N and P (Eq. A22) and growth
 258 of M (Eq. A29). Slower M growth causes slower mineralization (Eq. A26), and hence lowers
 259 aqueous concentrations of NH_4^+ , NO_3^- and $H_2PO_4^-$.

260 WTD drawdown can increase θ_g that results in greater D_g (Eq. D44) and more rapid
 261 gaseous O_2 transport. A consequent rise in $[O_{2s}]$ increases O_2 uptake (Eq. A17) and R_h (Eq. A14),
 262 R_g (Eq. A20) and growth of M (Eq. A25). Larger M hastens decomposition of organic C (Eqs.
 263 A1-A2) and production of DOC which further hastens R_h (Eq. A13), R_g and growth of M . More
 264 rapid decomposition of organic C under adequate $[O_{2s}]$ in this period also causes more rapid
 265 decomposition of organic N and P (Eq. A7) and production of DON and DOP, which increases
 266 uptake of microbial N and P (Eq. A22) and growth of M (Eq. A29). Rapid M growth causes rapid
 267 mineralization (Eq. A26), and hence greater aqueous concentrations of NH_4^+ , NO_3^- and $H_2PO_4^-$.

268 When WTD recedes below a certain threshold level, capillary rise from the WT can no
 269 longer support adequate recharge of the near surface peat layers and the surface litter (Eqs. D9,
 270 D12). It causes desiccation of the residue and the near surface peat layers thereby causing a
 271 reduction in water potential (ψ_s) and an increase in aqueous microbial concentrations ($[M]$) in



272 each of these layers (Eq. A15). Increased $[M]$ caused by the peat desiccation reduces microbial
273 access to the substrate for decomposition in each of the desiccated layers and reduces R_h (Eq.
274 A13). Reduction in R_h is calculated in *ecosys* from competitive inhibition of microbial exo-
275 enzymes with increasing concentrations (Eq. A4) (Lizama and Suzuki, 1991).

276 **2.1.3. WTD effects on vascular gross primary productivity**

277 *Ecosys* simulates effects of WTD variation on vascular GPP from WTD variation effects
278 on root O_2 and nutrient availability and root growth and uptake. Root O_2 and nutrient uptake in
279 *ecosys* are coupled with a hydraulically driven soil-plant-atmosphere water scheme. Root growth
280 in each vascular plant population in *ecosys* is calculated from its assimilation of the non-
281 structural C product of CO_2 fixation (σ_C) (Eq. C20). Assimilation is driven by R_g (Eq. C17)
282 remaining after subtracting R_m (Eq. C16) from autotrophic respiration (R_a) (Eq. C13) driven by
283 oxidation of σ_C (Eq. C14). Oxidation in roots may be limited by root O_2 reduction (Eq. C14b)
284 which is driven by root O_2 demand to sustain C oxidation and nutrient uptake (Eq. C14e), and
285 constrained by O_2 uptake controlled by concentrations of aqueous O_2 in the soil ($[O_{2s}]$) and roots
286 ($[O_{2r}]$) (Eq. C14d). Values of $[O_{2s}]$ and $[O_{2r}]$ are maintained by convective-dispersive transport
287 of O_2 through soil gaseous and aqueous phases and root gaseous phase (aerenchyma)
288 respectively and by dissolution of O_2 from soil and root gaseous to aqueous phases (Eqs. D39-
289 D45). O_2 transport through root aerenchyma depends on species-specific values used for root air-
290 filled porosity (θ_{pr}) (Eq. D45). Shallow WTD and resultant high peat moisture content in *ecosys*
291 can cause low θ_g that reduces soil O_2 transport, forcing root O_2 uptake to rely more on $[O_{2r}]$ and
292 hence on root O_2 transport determined by θ_{pr} . If this transport is inadequate, decline in $[O_{2r}]$
293 slows root O_2 uptake (Eqs. C14c-d) and hence R_a (Eq. C14b), R_g (Eq. C17) and root growth (Eq.
294 C20b) and root N and P uptake (Eqs. C23b, d, f). Root N and P uptake under shallow WT is



295 further slowed by reductions in aqueous concentrations of NH_4^+ , NO_3^- and H_2PO_4^- (Eqs. C23a,
 296 c, e) from slower mineralization of organic N and P. Slower root N and P uptake reduces
 297 concentrations of non-structural N and P products of root uptake (σ_N and σ_P) with respect to that
 298 of σ_C in leaves (Eq. C11), thereby slowing CO_2 fixation (Eq. C6) and GPP.

299 WTD drawdown facilitates rapid D_g which allows root O_2 demand to be almost entirely
 300 met from $[\text{O}_{2s}]$ (Eqs. C14c-d) and so enables more rapid root growth and N and P uptake (Eqs.
 301 C23b, d, f). Increased root growth and nutrient uptake is further stimulated by increased aqueous
 302 concentrations of NH_4^+ , NO_3^- and H_2PO_4^- (Eqs. C23a, c, e) from more rapid mineralization of
 303 organic N and P during deeper WT. Greater root N and P uptake increases concentrations of σ_N
 304 and σ_P with respect to σ_C in leaves (Eq. C11), thereby facilitating rapid CO_2 fixation (Eq. C6)
 305 and GPP. When WT falls below a certain threshold, inadequate capillary rise (Eqs. A9, A12)
 306 from deeper WT causes near-surface peat desiccation that reduces soil water potential (ψ_s) and
 307 raises soil hydraulic resistance (Ω_s) (Eq. B9), thereby forcing lower root water uptake (U_w) from
 308 desiccated layers (Eq. B6). However, deeper rooting facilitated by increased $[\text{O}_{2s}]$ under deeper
 309 WT can sustain U_w (Eq. B6) from wetter deeper peat layers with higher ψ_s and lower Ω_s (Eq.
 310 B9). If U_w from the deeper wetter layers cannot offset the suppression in U_w from desiccated
 311 near surface layers, the resultant net decrease in U_w causes a reduction in root, canopy and turgor
 312 potentials (ψ_r , ψ_c and ψ_t) (Eq. B4) and hence g_c (Eq. B2b) in *ecosys* when equilibrating U_w with
 313 transpiration (T) (Eq. B14). Lower g_c reduces CO_2 diffusion into the leaves thereby reducing CO_2
 314 fixation (Eq. C6) and GPP (Eq. C1).

315 **2.1.4. WTD effects on non-vascular gross primary productivity**

316 Effects of WTD drawdown on non-vascular (e.g., moss) GPP in *ecosys* is simulated from
 317 peat moisture supplying capacity through capillary rise from the WT to adequately recharge



318 shallow peat layers to sustain moss U_w . Tiny individuals of mosses with no stomatal regulation
319 are simulated in *ecosys* from intra-specific competition for light and nutrients (N, P) among large
320 moss populations. Simulated mosses in *ecosys* are mostly confined to near surface peat layers
321 that are frequently unsaturated. When WT deepens past a threshold level, inadequate capillary
322 rise (Eqs. D9, D12) causes near-surface peat desiccation, thereby reducing ψ_s and increasing Ω_s
323 (Eq. B9) of those layers. It causes a reduction in moss canopy water potential (ψ_c) while
324 equilibrating moss evaporation with moss U_w (Eq. B6). Reduced moss ψ_c causes a reduction in
325 moss carboxylation rate (Eqs. C3, C6a) and moss GPP (Eq. C1).

326 2.2. Modelling experiment

327 2.2.1. Study site

328 The algorithms for effects of WTD variations on ecosystem net CO₂ exchange in *ecosys*
329 were tested in this study against measurements of WTD and ecosystem net CO₂ fluxes at a flux
330 station of the Fluxnet-Canada Research Network established at the WPL (latitude: 54.95°N,
331 longitude: 112.47°W). The study site is a moderately nutrient-rich treed fen peatland within the
332 Central Mixed-wood Sub-region of Boreal Alberta, Canada. Peat depth around the flux station
333 was about 2 m. This peatland is dominated by stunted trees of black spruce (*Picea mariana*) and
334 tamarack (*Larix laricina*) with an average canopy height of 3 m. High abundance of a shrub
335 species *Betula pumila* (dwarf birch), and the presence of a wide range of mosses e.g., *Sphagnum*
336 spp., feather moss, and brown moss characterize the under-storey vegetation of WPL. The
337 topographic, climatic, edaphic and vegetative characteristics of this site were described in more
338 details by Syed et al. (2006).



339 2.2.2. Field data sets

340 *Ecosys* model inputs of half hourly weather variables i.e. incoming shortwave and
341 longwave radiation, air temperature (T_a), wind speed, precipitation and relative humidity during
342 2003-2009 were measured by Syed et al. (2006) and Flanagan and Syed (2011) at the
343 micrometeorological station installed at the WPL. To test the adequacy of WTD simulation in
344 *ecosys*, modelled outputs of hourly WTD were tested against WTD measured at the WPL with
345 respect to average hummock surface by Flanagan and Syed (2011). To examine how well *ecosys*
346 simulated net ecosystem CO₂ exchange at the WPL, we tested hourly modelled net ecosystem
347 CO₂ fluxes against those measured by using eddy covariance (EC) micro-meteorological
348 approach by Syed et al. (2006) and Flanagan and Syed (2011). Quality control, and gap-filling of
349 EC measured net CO₂ fluxes, and partitioning of EC-gap filled net CO₂ fluxes into GPP and R_e
350 were done by Syed et al. (2006) and Flanagan and Syed (2011).

351 Soil CO₂ fluxes measured by automated chambers can provide a valuable supplement to
352 EC CO₂ fluxes in testing modelled respiration by providing more continuous measurements than
353 EC. So, we also tested our modelled outputs against half-hourly automated chamber
354 measurements by Cai et al. (2010) at the WPL. These CO₂ flux measurements were carried out
355 over both hummocks and hollows by using a total of 9 steady-state transparent chambers (Cai et
356 al., 2010). Apart from soil respiration these chamber CO₂ fluxes thus included fixation and
357 autotrophic respiration from dwarf shrubs, herbs and mosses (Cai et al., 2010). Therefore we
358 compared modelled fixation and autotrophic respiration from understory PFTs (e.g., shrub and
359 moss) combined with modelled soil respiration against these chamber net CO₂ fluxes measured
360 at the WPL. For this purpose net CO₂ flux measurements from all of those chambers were



361 averaged and compared against average soil and understorey CO₂ fluxes modelled over the
362 hummock and the hollow.

363 **2.2.3. Model run**

364 *Ecosys* model run to simulate WTD effects on net CO₂ exchange of WPL had a
365 hummock and a hollow grid cell that exchanged water, heat, carbon and nutrients (N, P) between
366 them and with surrounding vertical and lateral boundaries (Fig. 1). The hollow grid cell had near
367 surface peat layer that was 0.3 m thinner than the hummock cell representing a hummock-hollow
368 surface difference of 0.3 m observed in the field (Long, 2008) (Fig. 1). Any depth with respect to
369 the modelled hollow surface would thus be 0.3 m shallower than the depth with respect to the
370 modelled hummock surface.

371 Peat organic and chemical properties at different depths of the WPL were represented in
372 *ecosys* by inputs from measurements either at the site (e.g., Syed et al., 2006; Flanagan and Syed,
373 2011) or at similar nearby sites (e.g., Rippey and Nelson, 2007) (Fig. 1). However, we did not
374 have any site measurement for the nutrient gain through lateral water inflow which was observed
375 by Syed et al. (2006) during the field measurements. Instead, we used background wet deposition
376 rates of 0.5 mg ammonium-N, 0.25 mg nitrate-N and 0.075 mg phosphate-P per litre of
377 precipitation water to simulate an additional source of nutrient input.

378 *Ecosys* was run for a spin up period of 1961-2002 under repeating 7-year sequences of
379 hourly weather data (shortwave and longwave radiation, air temperature, wind speed, humidity
380 and precipitation) recorded at the site from 2003 to 2009. There was a drying trend observed
381 from 2003 to 2009 due to diminishing precipitation that caused WTD drawdown in the
382 watershed in which WPL is located, which lowered the WT of this fen peatland (Flanagan and



383 Syed, 2011). To accommodate the gradual drying effects of catchment hydrology on modelled
384 fen peatland WTD, we set the WTD_x at different levels based on the annual wetness of weather,
385 e.g., shallow, intermediate, and deep ($WTD_x=0.19, 0.35$ and 0.72 m below the hummock surface,
386 or 0.11 m above and 0.05 and 0.42 m below the hollow surface) (Fig. 1). There was no exchange
387 of water through lower model boundary to represent the presence of nearly impermeable clay
388 sediment underlying the peat (Syed et al., 2006) (Fig. 1). Variations in peat surface with WTD
389 variations, which is an important hydrologic self-regulation of boreal peatlands (Dise, 2009), was
390 not represented in this version of *ecosys*.

391 At the start of the spin up run, the hummock grid cell was seeded with an evergreen
392 needle leaf and a deciduous needle leaf over-storey plant functional types (PFT) to represent the
393 black spruce and tamarack trees at the WPL. The hollow grid cell was seeded with only the
394 deciduous needle leaf over-storey PFTs since the black spruce trees at the WPL only grew on the
395 raised areas. Each of the modelled hummock and the hollow was also seeded with a deciduous
396 broadleaved vascular (to represent dwarf birch) and a non-vascular (to represent mosses) under-
397 storey PFTs. The planting densities were such that the population densities of the black spruce,
398 tamarack, dwarf birch and moss PFTs were $0.16, 0.14, 0.3,$ and 500 m^{-2} respectively at the end of
399 the spin up run so as to best represent field vegetation (Syed et al., 2006; Mezbahuddin et al.,
400 2016). To include wetland adaptation, we used a root porosity (θ_{pr}) value of 0.1 for the two over-
401 storey PFTs and a higher θ_{pr} value of 0.3 for the under-storey vascular PFT to represent better
402 wetland adaptation in the under-storey than the over-storey PFTs. These θ_{pr} values were used in
403 calculating root O_2 transport through aerenchyma (Eq. D45) and did not change with
404 waterlogging throughout the model run. These θ_{pr} values were representatives of root porosities
405 measured for various northern boreal peatland plant species (Cronk and Fennessy, 2001). Non-



406 symbiotic N₂ fixation through association of cyanobacteria and mosses are also reported for
407 Canadian boreal forests (Markham, 2009). This was represented in *ecosys* as N₂ fixation by non-
408 symbiotic heterotrophic diazotrophs (Eq. A27) in the moss canopy. Further details about *ecosys*
409 model set up to represent the hydrological, physical and ecological characteristics of WPL can be
410 found in Mezbahuddin et al. (2016).

411 When the modelled ecosystem attained stable values of net ecosystem CO₂ exchange at
412 the end of the spin-up run, we continued the spin up run into a simulation run from 2003 to 2009
413 by using a real-time weather sequence. We tested our outputs from 2004-2009 of the simulation
414 run against the available site measurements of WTD, net EC CO₂ fluxes and net chamber CO₂
415 fluxes over those years.

416 2.2.4. Model validation

417 To examine the adequacy of modelling WTD effects on canopy, root and soil CO₂ fluxes
418 which were summed for net ecosystem CO₂ exchange at the WPL, we spatially averaged hourly
419 net CO₂ fluxes modelled over the hummock and the hollow to represent a 50:50 hummock-
420 hollow ratio and then regressed against hourly EC measured net ecosystem CO₂ fluxes for each
421 year from 2004-2009 with varying WTD. Each of these hourly EC measured net ecosystem CO₂
422 fluxes used in these regressions is an average of two half-hourly net CO₂ fluxes measured at a
423 friction velocity (u^*) greater than 0.15 m s⁻¹. Model performance was evaluated from regression
424 intercepts ($a \rightarrow 0$), slopes ($b \rightarrow 1$), coefficients of determination ($R^2 \rightarrow 1$), and root means squares
425 for errors (RMSE $\rightarrow 0$) for each study year to test whether there was any systematic divergence
426 between the modelled and EC measured CO₂ fluxes. Similar regressions of modelled vs. gap-
427 filled net CO₂ fluxes were also performed to test for any divergence between the modelled and
428 gap-filled CO₂ fluxes. These regressions based tests are very important since any small



429 divergence between hourly modelled and EC measured as well as between hourly modelled and
430 gap-filled CO₂ fluxes can result in a large divergence between modelled and EC-gap filled
431 annual estimates.

432 **2.2.5. Sensitivity of modelled peatland CO₂ exchange to artificial drainage**

433 Large areas of northern boreal peatlands in Canada have been drained primarily for
434 increased forest and agricultural production since plant productivity in pristine peatlands are
435 known to be constrained by shallow WTD (Choi et al., 2007). Drainage and resultant WTD
436 drawdown can affect both GPP and R_e on a short-term basis and the vegetation composition on a
437 longer time scale thereby changing overall net CO₂ exchange trajectories of a peatland. To
438 predict short-term effects of drainage on WTD and hence ecosystem net CO₂ exchange of WPL,
439 we extended our simulation run into a projection run consisting two 7-yr cycles by using
440 repeated weather sequences of 2003-2009. While doing so, we forced a stepwise drawdown in
441 WTD_x by 1.0 and 2.0 m from that used in spin-up and simulation runs (Fig. 1) in the first
442 (drainage cycle 1) and the second cycle (drainage cycle 2) respectively. This projection run
443 would give us a further insight about how the northern boreal peatland of Western Canada would
444 be affected by further WTD drawdown as a result of drier and warmer weather as well as a
445 disturbance such as drainage. It would also provide us with a test of how sensitive the modelled
446 C processes were to the changes in model lateral boundary condition as defined by WTD_x in
447 *ecosys*.

448 **3. Results**

449 **3.1. Model performance in simulating diurnal variations in ecosystem net CO₂ fluxes**

450 Variations in precipitation can cause change in WTD and consequent variation in diurnal
451 net CO₂ exchange across years. *Ecosys* simulated diurnal net CO₂ fluxes reasonably well which



452 was measured each year from 2004 to 2008 with varying precipitation (Table 1). On a year-to-
453 year basis, regressions of hourly modelled vs. measured net ecosystem CO₂ fluxes gave
454 intercepts within 0.1 μmol m⁻² s⁻¹ of zero, and slopes within 0.1 of one, indicating minimal bias
455 in modelled outputs during each year from 2004-2008 (Table 1). On a growing season (May-
456 August) basis, regressions of modelled on measured hourly net CO₂ fluxes yielded larger
457 positive intercepts from 2004-2009 (Table 2). The larger intercepts were predominantly caused
458 by modelled overestimation of growing season day-time CO₂ fluxes. This overestimation was
459 offset by modelled overestimation of night-time CO₂ fluxes during the winter thus yielding
460 smaller intercepts from throughout-the-year regressions of modelled vs. EC measured fluxes
461 (Tables 1 vs. 2). We could not do a modelled vs. EC CO₂ regression for the entire year of 2009
462 due to the lack of flux measurements from September to December in that year. Values for
463 coefficients of determination (R^2) were ~ 0.8 ($P < 0.001$) for all years from both throughout-the-
464 year and growing season regressions (Tables 1 and 2). RMSEs were < 2.0 and ~2.5 μmol m⁻² s⁻¹
465 for whole year regressions from 2004-2008 (Table 1) and for growing season regressions from
466 2004-2009 (Table 2) respectively. Much of the variations in EC measured CO₂ fluxes that was
467 not explained by the modelled fluxes could be attributed to a random error of ~20% in EC
468 methodology (Wesely and Hart, 1985). This attribution was further corroborated by root mean
469 squares for random errors (RMSRE) in EC measurements, calculated for forests with similar
470 CO₂ fluxes from Richardson et al. (2006) that were similar to RMSE (Table 1). The similar
471 values of RMSE and RMSRE also indicated that further constraint in model testing could not be
472 achieved without further precision in EC measurements.

473 Regressions of modelled vs. gap-filled CO₂ fluxes gave slopes and R^2 which were similar
474 to, and RMSEs which were smaller than those from modelled vs. EC-measured CO₂ fluxes for



475 most of the years except for the throughout-the-year regressions in 2004 and 2006 when the
476 slopes were larger (Tables 1 and 2). The intercepts from modelled vs. gap filled CO₂ fluxes were
477 consistently more negative than those from modelled vs. EC measured fluxes for both whole
478 year (Table 1) and growing season (Table 2) regressions. It was mainly caused by larger
479 modelled than gap filled night-time CO₂ effluxes.

480 **3.2. Seasonality in WTD and net ecosystem CO₂ exchange**

481 Seasonality in WTD measured at the WPL showed interannual variation from 2004 to
482 2009 which was modelled reasonably well by *ecosys* (Figs. 2b, d, f, h, j, l). The interannual
483 variation in seasonality of WTD was modelled by adequate simulation of the balance between
484 vertical water fluxes i.e., precipitation vs. evapotranspiration and lateral water fluxes i.e.,
485 recharge vs. discharge. Larger precipitation to evapotranspiration ratio (P/ET) throughout 2004
486 caused the shallowest modelled WTD which remained above the hollow surface throughout most
487 of the year (Fig. 2b). $WTD_x (=0.19\text{ m})$ (Fig. 1) shallower than the modelled WTD in 2004
488 created a hydraulic gradient that caused net lateral recharge and hence further sustained the
489 shallow modelled WTD. A smaller P/ET in 2005 than in 2004 caused slightly deeper WTD that
490 remained at the hollow surface or within 0.1 m below the hollow surface (Fig. 2d). During this
491 year, $WTD_x (=0.19\text{ m})$ (Fig. 1) shallower than the modelled WTD caused net lateral recharge and
492 hence further sustained WTD close to the hollow surface. Declines in the P/ET over the growing
493 seasons of 2006 and 2007 caused modelled WTD drawdown to levels where the differences
494 between evapotranspiration and precipitation equilibrated with net lateral recharge caused by
495 hydraulic gradients yielded from $WTD_x (=0.35\text{ m})$ (Fig. 1) which was deeper than the modelled
496 WTD in both years (Figs. 2f, h). Continued declines in growing season P/ET in 2008 and 2009
497 caused further deepening of the WT (Figs. 2j, l). A $WTD_x (=0.72\text{ m})$ (Fig. 1) deeper than the



498 modelled WTD in these growing seasons generated hydraulic gradients that caused net lateral
499 discharge which further deepened WT. Above mentioned modelled interannual variations in
500 seasonality of WTD from 2004 to 2009 were well corroborated by site measured half hourly
501 WTD at the WPL (Figs. 2b, d, f, h, j, l).

502 Seasonality in net CO₂ exchange at the WPL was predominantly governed by that in
503 temperature which controlled the seasonality in phenology and GPP as well as that in *R_e*. *Ecosys*
504 simulated the seasonality in phenology and hence GPP, and *R_e* reasonably well during a gradual
505 growing season WTD drawdown from 2004 to 2009 which was apparent by good agreements
506 between modelled vs. EC-gap filled daily NEP (Fig. 2) and hourly net CO₂ fluxes (Tables 1 and
507 2). Modelled NEP throughout the winters of most of the years were more negative than the EC-
508 gap filled NEP indicating larger modelled than EC-gap filled winter CO₂ effluxes (Fig. 2). This
509 trend was also indicated by negative intercepts from throughout-the-year regressions of modelled
510 vs. gap-filled CO₂ fluxes (Table 1). The onset of photosynthesis at the WPL varied interannually
511 depending upon spring temperature which was also modelled adequately by *ecosys*. For instance,
512 2004 with a cooler spring produced smaller early growing season (May) GPP and hence NEP
513 than 2005 with a warmer spring which was apparent in daily EC-gap filled and modelled NEP
514 (Figs. 2a vs. 2c).

515 3.3. WTD effects on diurnal net ecosystem CO₂ exchange

516 WTD variation can affect diurnal net CO₂ exchange by affecting peat O₂ status and
517 consequently root and microbial O₂ and nutrient availability, growth and uptake thereby
518 influencing CO₂ fixation and/or respiration. To examine modelled vs. measured WTD effects on
519 diurnal net CO₂ exchange at the WPL, we examined three 10-day periods with comparable
520 weather conditions (radiation and air temperature) that differed predominantly in their WTD



521 during late growing seasons (August) of 2005, 2006 and 2008 (Fig. 3). A WTD drawdown from
522 late growing season of 2005 to that of 2006 in *ecosys* caused a reduction in peat water contents
523 and a consequent increase in O₂ influxes from atmosphere into the peat that eventually caused an
524 increase in modelled soil CO₂ effluxes (Fig. 4c). Increased modelled soil CO₂ effluxes in mid-
525 August of 2006 contributed to the larger modelled ecosystem CO₂ effluxes (R_e) as apparent in
526 larger modelled night-time fluxes in the late growing season of 2006 than in that of 2005 which
527 was well corroborated by night-time EC CO₂ fluxes during those periods (Fig. 4a). The
528 stimulation of R_e as a result of WTD drawdown was further corroborated by larger sums of
529 night-time soil CO₂ fluxes and understorey autotrophic respiration (R_a) as measured by Cai et al.
530 (2010) using automated chambers and modelled by *ecosys* in late growing season of 2006 with
531 deeper WTD than in that of 2005 with shallower WTD (Fig. 4b).

532 Further WTD drawdown into the late growing season of 2008 (Fig. 3c) caused improved
533 peat oxygenation and hence larger soil CO₂ effluxes in the model (Fig. 4c). It contributed to
534 similarly larger modelled night-time CO₂ fluxes in the late growing seasons of 2006 and 2008
535 than in 2005 that were also well corroborated by EC measured night-time fluxes during those
536 periods (Fig. 4a). Consequently, the sums of modelled night-time soil CO₂ fluxes and
537 understorey R_a in late growing season of 2008 were similarly larger as in 2006 with respect to
538 those in that period of 2005 (Fig. 4b). We did not have any chamber measurements available for
539 2008 to corroborate the modelled outputs. Despite larger night-time modelled and EC CO₂ fluxes
540 in the late growing season of 2008 than in 2005, the day-time influxes in 2008 were also similar
541 to those in 2005 (Fig. 4a). It indicated a greater late growing season CO₂ fixation with WTD
542 drawdown from 2005 to 2008. WTD drawdown thus stimulated both the night-time and the day-
543 time net CO₂ fluxes as apparent in both the modelled outputs and in EC flux measurements



544 during the three WTD conditions mentioned above thereby indicating increases in both R_e and
545 GPP with the deepening of WT.

546 Apart from WTD, temperature variation could also profoundly affect ecosystem net CO₂
547 exchange at the WPL. For a given WTD condition, warmer weather caused increases in R_e at the
548 WPL (Figs. 3b-c and 4a-b). Larger night-time modelled, EC-gap filled and chamber CO₂ fluxes
549 in warmer nights of day 214, 220 and 222 than the cooler nights of day 221, 224 and 218 in
550 2005, 2006 and 2008 respectively indicated the trend of increased R_e with warming under similar
551 WTD condition (Figs. 3b and 4a-b). However, at similar temperature conditions, modelled and
552 EC-gap filled night-time ecosystem CO₂ fluxes as well as modelled and chamber measured sums
553 of night-time soil CO₂ fluxes and understorey R_a under deeper WT in 2006 and 2008 were larger
554 than those in 2005 under shallower WT (denoted by the grey arrows in Figs. 3b and 4a-b). It
555 indicated R_e stimulation as a result of WTD drawdown at the WPL regardless of temperature
556 condition that further corroborated the net effects of WTD drawdown on R_e and hence on net
557 ecosystem CO₂ exchange.

558 The degree of stimulation in R_e at the WPL due to warming was also influenced by WT
559 conditions. To study this effect we further examined three 4-day warming events in late July and
560 early to mid-August of 2005, 2006 and 2008 with gradually deeper WT (Figs. 5a-f). The
561 warming events in early to mid-August of 2006 and 2008, when WT was deeper than in late July
562 of 2005, caused gradual increases in R_e as apparent from gradually larger modelled and EC-gap
563 filled night-time ecosystem CO₂ effluxes (Figs. 5h-i). Increases in R_e due to warming under
564 deeper WT were also apparent in gradually larger modelled and sums of chamber-measured
565 night-time soil CO₂ fluxes and understorey R_a in 2006 and modelled understorey and soil CO₂
566 fluxes in 2008 (Figs. 5k-l). This R_e stimulation due to warming under deeper WT contributed to



567 declines in modelled and EC-gap filled July-August NEP in 2006 and 2008 (Figs. 2e, i). Unlike
568 in 2006 and 2008, a late-July warming event in 2005 with shallower WT did not yield a similarly
569 evident stimulation of either modelled or EC-gap filled R_e and either modelled or chamber
570 measured soil and understorey respiration (Figs. 5g, j). Lack of stimulation in R_e with warming
571 under shallower WT in 2005 resulted in the absence of decline in July-August NEP as occurred
572 in 2006 and 2008 (Figs. 2c vs. 2e, i). These findings thus showed that the stimulation of R_e due to
573 warming was greater with deeper WT thereby further indicating importance of WTD in
574 mediating potential future warming effects on NEP of northern boreal peatlands.

575 **3.4. Interannual variations in WTD and net ecosystem productivity**

576 The effects of WTD drawdown on modelled and EC-gap filled diurnal net ecosystem
577 CO_2 exchange also contributed to the effects of interannual variation in WTD on that of NEP.
578 *Ecosys* simulated a gradual drawdown of average growing season (May-August) WTD from
579 2004 to 2009 from gradually declining growing season P/ET and lateral water gain through
580 recharge (Fig. 6d). Simulated WTD drawdown was corroborated well by site measured WTD at
581 the WPL (Fig. 6d). Slightly deeper WT in 2005 than in 2004 caused larger growing season GPP
582 in *ecosys* that was corroborated by EC-derived GPP (Fig. 6b). The increase in GPP from 2004 to
583 2005 was also contributed by larger GPP in warmer May of 2005 than 2004. Slight WTD
584 drawdown from 2004 to 2005 did not raise either modelled or EC-derived growing season R_e
585 (Fig. 6c). It was because of June and July in 2005 being more than 2°C cooler than in 2004
586 thereby causing cooler soil which reduced R_e . Reduction in June and July R_e due to cooler soil
587 more than fully offset the increase in R_e due to slight WTD drawdown and resulted in decreased
588 growing season modelled and EC-derived R_e in 2005 than in 2004 (Fig. 6c). Larger GPP and
589 smaller R_e together caused a larger growing season NEP in 2005 than in 2004 (Fig. 6a).



590 WTD drawdown in *ecosys* from 2005 to 2006 caused increases in both modelled growing
591 season GPP and R_e that was corroborated by EC-derived GPP and R_e (Figs. 6b-c). Increases in
592 GPP and in R_e with deepening of WT from 2005 to 2006 were also apparent in modelled vs. EC-
593 gap filled and chamber diurnal net CO₂ fluxes (Figs. 4-5). Warmer growing season in 2006 than
594 in 2005 (Fig. 6d) caused warmer soil that further contributed to the increase in modelled and EC-
595 derived growing season R_e from 2005 with shallower WT to 2006 with deeper WT (Figs. 4, 5
596 and 6c-d). A larger increase in growing season R_e than that in GPP caused modelled and EC-
597 derived growing season NEP to decrease from 2005 to 2006 (Fig. 6a). Continued growing season
598 WTD drawdown from 2006 to 2008 caused similar increases in modelled growing season GPP
599 and R_e that caused no significant changes in modelled growing season NEP (Figs. 6a-d). Like the
600 modelled estimates, EC-derived growing season GPP and R_e also increased with WTD
601 drawdown from 2006 to 2008 (Figs. 6a-d). However, the rate of increase in EC-derived growing
602 season R_e was smaller than that in modelled growing season R_e thereby contributing to a larger
603 growing season EC-gap filled NEP in 2008 than in 2006 which was not apparent in modelled
604 estimates (Figs. 6a-c). A further drawdown in WTD from the growing season of 2008 to 2009
605 caused reductions in both modelled and EC-derived growing season GPP and R_e (Figs. 6a-d).
606 Reductions in GPP and R_e from 2008 to 2009 could also be contributed by lower T_a in 2009 than
607 in 2008 that caused cooler canopies and soil (Figs. 6b-d). The reduction in EC-derived growing
608 season GPP was larger than that in EC-derived growing season R_e thereby causing a decrease in
609 growing season EC-gap filled NEP from 2008 to 2009 (Figs. 6a- c). On the contrary, the
610 reduction in modelled growing season GPP from 2008 to 2009 was less than that in the EC-
611 derived GPP thereby causing an increase in modelled growing season NEP from 2008 to 2009
612 (Figs. 6a-c).



613 Despite the counteracting and offsetting effects of WTD and T_a on GPP and R_e , larger
614 modelled and EC-derived estimates of growing season GPP and R_e in 2009 than in 2004 with
615 similar mean T_a suggested that both modelled and EC-derived growing season GPP and R_e
616 increased with the deepening of average growing season WT at the WPL (Figs. 6a-d). It was
617 further corroborated by polynomial regressions of modelled growing season estimates of GPP
618 and R_e on modelled average growing season WTD and similar regressions of EC-derived
619 growing season GPP and R_e on measured average growing season WTD (Figs. 7a-c). The
620 relationships showed that there were increases in modelled and EC-derived growing season GPP
621 and R_e with deepening of the growing season WT from 2004 to 2008 after which further WTD
622 drawdown in 2009 started to cause slight declines in both GPP and R_e (Figs. 7b-c). Neither
623 modelled nor EC-gap filled estimates of growing season NEP yielded significant regressions
624 when regressed on modelled and measured growing season WTD respectively (Fig. 7a). It
625 indicated that similar increases in modelled and EC-derived growing season estimates of GPP
626 and R_e with deepening of WT along with some counteracting effects of T_a left no net effects of
627 WTD drawdown on either modelled or EC-derived growing season NEP (Figs. 6 and 7a).

628 WTD effects on growing season GPP and R_e and hence NEP from 2004 to 2009 as
629 measured at the WPL and modelled by *ecosys* were also consistent at an annual time scale from
630 2004 to 2008 (Figs. 6e-h). Similar to the growing season trend, drawdown of both measured and
631 modelled WTD averaged over the ice free periods (May-October) from 2004 to 2008 stimulated
632 annual modelled and EC-derived GPP (Figs. 6f, h and 7e). The deepening of WT also raised
633 modelled and EC-derived annual R_e from 2005 to 2008 as was in the case of growing season R_e
634 (Figs. 6g-h and 7f). Similar increases in both modelled and EC-derived annual GPP and R_e with
635 WTD drawdown left no net WTD effects on modelled and EC-gap filled annual NEP (Fig. 7d).



636 We did not include the year 2009 while examining the effects of WTD drawdown on interannual
637 variation of GPP, R_e and NEP due to the lack of EC CO₂ flux measurements from September to
638 December in 2009 (Figs. 6e-h and 7d-f). Even though, modelled WTD effects on GPP, R_e and
639 hence NEP were corroborated well by EC-derived GPP, R_e and EC-gap filled NEP, the modelled
640 growing season and annual GPP and R_e were consistently higher than the EC-derived estimates
641 of those from 2004 to 2009 (Figs. 6-7).

642 Increased GPP with WTD drawdown (Figs. 6b, f and 7b, e) was modelled by *ecosys*
643 predominantly through increased root growth and uptake of nutrients and consequently improved
644 leaf nutrient status and hence more rapid CO₂ fixation in vascular PFTs. Under shallow WT
645 during the growing season of 2004, roots in modelled black spruce PFT hardly grew below 0.35
646 m from the hummock surface (black spruce was not planted in the hollow) and the roots of
647 modelled tamarack PFT were mostly confined within 0.35 m below the hummock surface and
648 0.05 m below the hollow surface. Modelled root densities of both black spruce and tamarack
649 were higher by 2-3 orders of magnitude in the top 0.19 m of the hummock (data not shown). A
650 WTD drawdown from ~0.05 m above the hollow surface (~0.25 m below the hummock surface)
651 in the growing season of 2004 to ~0.35 m below the hollow surface (~0.65 m below the
652 hummock surface) in the growing season of 2009 caused an increase in maximum modelled
653 rooting depth from 0.35 to 0.65 m below the hummock surface in black spruce and from 0.35 to
654 0.65 m below the hummock and from 0.05 to 0.35 m below the hollow surface in the tamarack
655 PFT. Increased root growth in modelled vascular PFTs augmented root surface area for nutrient
656 uptake under deeper WT in the growing season of 2009 than in 2004. Increased root surface area
657 along with increased nutrient availability due to more rapid mineralization with improved
658 aeration as a result of WTD drawdown from 2004 to 2009 caused improved root nutrient uptake



659 in modelled vascular PFTs. Increased root growth, nutrient availability and hence uptake due to
660 WTD drawdown from the growing season of 2004 to that of 2009 in *ecosys* caused an increase in
661 modelled foliar N concentrations in black spruce, tamarack and dwarf birch PFTs from 14, 32,
662 and 37 g N kg⁻¹ C to 17, 37 and 45 g N kg⁻¹ C respectively, driving the increases in GPP
663 modelled over this period (Figs. 6b, f and 7b, e). The modelled foliar N concentrations in the
664 growing season of 2004 were well corroborated by the foliar N concentrations of 12, 33 and 41 g
665 N kg⁻¹ C for black spruce, tamarack and dwarf birch as measured by Syed et al. (2006) during
666 summer 2004 at our study site.

667 **3.5. Simulated drainage effects on WTD and NEP**

668 Artificial drainage can drastically alter the WTD in a peatland that can cause dramatic
669 changes in peatland NEP by shifting the balance between GPP and R_e . To predict drainage
670 effects on WTD and hence C balance of WPL, we performed a projected drainage simulation in
671 *ecosys* with two additional 7-year weather cycles (Sect. 2.2.5). This drainage simulation would
672 also serve as a climate change analog in providing us insight into how potential WTD drawdown
673 under future drier and warmer climates would affect boreal peatland GPP, R_e and hence NEP.
674 Forcing WTD_x deeper by 1 and 2 m in the drainage cycles 1 and 2 lowered growing season WT
675 by ~0.5 m and ~0.55 m respectively from those in the real-time simulation in all the years from
676 2004 to 2009 (Fig. 8a).

677 The projected drawdown of growing season WTD in *ecosys* caused changes in modelled
678 growing season NEP, GPP and R_e . Modelled growing season GPP increased with drainage-
679 induced WTD drawdown up to ~0.5 m below the hollow surface (~0.8 m below the hummock
680 surface) below which GPP decreased (Figs. 8c, f). The WTD drawdown affected modelled
681 vascular and non-vascular growing season GPP quite differently. Modelled growing season



682 vascular GPP increased with WTD drawdown before it plateaued and eventually decreased when
683 WTD fell below ~ 0.6 m from the hollow surface (~ 0.9 m below the hummock surface) (Figs. 9a,
684 c, e). On the contrary, modelled non-vascular growing season GPP continued to decrease with
685 WTD drawdown below ~ 0.1 m from the hollow surface (~ 0.4 m below the hummock surface)
686 (Figs. 9a-b, d).

687 WTD drawdown due to simulated drainage not only affected modelled growing season
688 GPP but also affected, and was affected by, the associated change in evapotranspiration. Deeper
689 WTD_x in drainage cycle 1 caused larger hydraulic gradients and greater lateral discharge thereby
690 deepening the WT with respect to that in the real-time simulation (Figs. 8a). Larger GPP
691 throughout the growing seasons of 2004-2007 in the drainage cycle 1 than in the real-time
692 simulation caused a greater vertical water loss through evapotranspiration that further
693 contributed to this deepening of WT (Fig. 8b). However, greater lateral water discharge in
694 drainage cycle 2 caused by deeper WTD_x did not deepen the modelled growing season WT much
695 below that in cycle 1 (Fig. 8a). The larger lateral water loss through discharge in drainage cycle 2
696 than in cycle 1 was mostly offset by slower vertical water losses through evapotranspiration as
697 indicated by smaller GPP in the drainage cycle 2 (Fig. 8b). The changing feedbacks between
698 WTD and GPP and hence evapotranspiration in *ecosys* also indicated the ability of the model to
699 simulate hydrological self-regulation which is an important characteristic of peatland eco-
700 hydrology (Dise, 2009).

701 Modelled growing season R_e continued to increase with deepening of modelled WT due
702 to drainage (Figs. 8d, g). Reductions in modelled growing season R_e from drainage cycle 1 to 2
703 during 2006-2009 indicated R_e inhibition due to desiccation of near surface peat layers and
704 surface residues (Fig. 8d). Overall larger increases in GPP than those in R_e with initial WTD



705 drawdown in the drainage simulation slightly increased modelled growing season NEP (Figs. 8
706 b, e). Continued WTD drawdown in the drainage simulation caused declines in GPP particularly
707 in model years of 2008 and 2009 while causing greater R_e or a smaller decline in R_e than in GPP,
708 thereby causing declines in NEP (Figs. 8b-d). The projected drainage simulation effect on WTD
709 and NEP in *ecosys* may reflect short-term drainage effects and hence may be transient. Long-
710 term manipulation of WTD through drainage may produce different trajectories of WTD effects
711 on C processes and plant water relations in northern boreal peatlands via vegetation adaptation
712 and succession (Strack et al., 2006; Munir et al., 2014).

713 4. Discussion

714 4.1. Modelling WTD effects on northern boreal peatland NEP

715 Modelled and EC-gap filled diurnal, seasonal and annual NEP, GPP and R_e vs. modelled
716 and observed WTD suggested that WTD drawdown raised both GPP and R_e at the WPL (Figs. 2-
717 7). Similar increases in GPP and R_e with WTD drawdown along with some offsetting effects of
718 T_a yielded no net effect of WTD drawdown on NEP at the WPL during 2004-2009 (Figs. 6-7).
719 The simulated drainage experiment in *ecosys* suggested that the increase in GPP would diminish
720 and eventually shift to a decrease in GPP should WT fall further below a threshold of about
721 ~0.45 m from the hollow surface, particularly during drier years (Figs. 8c, f and 9). The decrease
722 in GPP would also be accompanied by increased R_e thereby causing a decrease in NEP should
723 the deepening of WT continue at the WPL (Figs. 8b, d-e, g). Our hypotheses that describe how
724 *ecosys* would simulate above mentioned WTD effects on R_e , GPP and NEP at the WPL are
725 discussed in the following sections of 4.1.1 to 4.1.4.



726 4.1.1. Hypothesis 1: Increase in R_e with WTD drawdown

727 Shallow WTD in *ecosys* caused shallow aerobic zone above WT and thicker anaerobic
728 zone below the WT. In the shallow aerobic zone, peat O_2 concentration [O_{2s}] was well above the
729 Michaelis-Menten constant for O_2 reduction ($K_m=0.064 \text{ g m}^{-3}$) and hence DOC oxidation and
730 consequent microbial uptake and growth in *ecosys* was not much limited by [O_{2s}] (Eqs. A17a,
731 C14c). On the contrary, [O_{2s}] in the thicker anaerobic zone below the WT was well below K_m so
732 that DOC oxidation was coupled with DOC reduction by anaerobic heterotrophic fermenters,
733 which yielded much less energy ($4.4 \text{ kJ g}^{-1} \text{ C}$) than did DOC oxidation coupled with O_2
734 reduction ($37.5 \text{ kJ g}^{-1} \text{ C}$) (Eq. A21). Lower energy yields in the thicker anaerobic zone resulted in
735 slower microbial growth (Eq. A25) and R_h (Eq. A13). Since the anaerobic zone in *ecosys* was
736 thicker than the aerobic zone under shallow WT, lower modelled R_h in the anaerobic zone
737 contributed to reduced modelled soil respiration and hence R_e that was corroborated by EC
738 measurements at the WPL (Figs. 4-7). WTD drawdown in *ecosys* caused peat pore drainage and
739 increased θ_g thereby deepening of the aerobic zone. It raised D_g (Eq. D44) and increased O_2
740 influxes into the peat (Fig. 4c) (Eqs. D42-D43). Increased O_2 influxes enhanced [O_{2s}] and
741 stimulated R_h (Eqs. A13, A20), soil respiration and hence R_e (Figs. 4-7). Rapid mineralization of
742 DON and DOP due to improved [O_{2s}] under deeper WT also raised aqueous concentrations of
743 NH_4^+ , NO_3^- and $H_2PO_4^-$ (Eqs. C23a, c, e) that increased microbial nutrient availability, uptake
744 (Eq. A22) and growth (Eq. A29) and further enhanced R_e (Figs. 4-7).

745 The modelling hypothesis of increased R_e stimulated by improved peat oxygenation due
746 to WTD drawdown can be corroborated by other field, laboratory and modelling studies on
747 similar peatlands. Automated chamber measurements by Cai et al. (2010) at our study site
748 showed increased soil respiration with deeper WT thereby further corroborating our hypothesis



749 (Figs. 4b and 5j-l). Kotowska (2013) found through a combination of automated chamber
750 measurements and a laboratory incubation study that increases in aerobic microbial
751 decomposition stimulated by WTD drawdown contributed to higher R_e in a moderately rich fen
752 very close to our study site. Mäkiranta et al. (2009) also found increased rates of microbial
753 decomposition in a Finish peatland due to thicker aerobic zone and consequently larger amounts
754 of decomposable organic matter exposed to aerobic oxidation.

755 Modelled increase in R_e of $0.26 \mu\text{mol CO}_2 \text{ m}^{-2} \text{ s}^{-1}$ per 0.1 m of WTD drawdown was
756 greater than the EC-derived R_e increase of $0.16 \mu\text{mol CO}_2 \text{ m}^{-2} \text{ s}^{-1}$ per 0.1 m WTD drawdown
757 reported by Flanagan and Syed (2011) for WPL over the growing seasons of 2004-2009 (Figs.
758 6c-d). The modelled rate of increasing R_e was, however, comparable with that of $\sim 0.3 \mu\text{mol m}^{-2}$
759 s^{-1} per 0.1 m of WTD drawdown estimated by Peichl et al. (2014) from EC-derived R_e over the
760 growing seasons of 2001-2012 in a Swedish fen. Ballantyne et al. (2014) also reported an
761 increase in EC-derived R_e of $\sim 0.33 \mu\text{mol m}^{-2} \text{ s}^{-1}$ per 0.1 m of WTD drawdown from a WTD
762 manipulation study in a Michigan peatland thereby further corroborating our modelling
763 hypothesis of increased R_e due to WTD drawdown.

764 Apart from WTD, peat warming in *ecosys* also increased rates of decomposition (Eq. A1)
765 through an Arrhenius function (Eq. A6) and increased R_h and R_e (Figs. 3-6). Warming effect on
766 decomposition in *ecosys* was also modified by WTD. For a similar warming, greater thermal
767 diffusivity in peat with deeper WT and consequent smaller water contents caused greater peat
768 warming (Eqs. D34, D36). It enabled *ecosys* to simulate larger increases in R_e during warming
769 periods in 2006 and 2008 with deeper WT than in 2005 (Figs. 3-5). Increased stimulation of peat
770 decomposition by warming under deeper WT was also modelled by Grant et al. (2012) using the



771 same model *ecosys* over a northern fen peatland at Wisconsin, USA and by Ise et al. (2008)
772 using a land surface scheme named ED-RAMS (Ecosystem Demography Model version 2
773 integrated with the Regional Atmospheric Modeling System) coupled with a soil biogeochemical
774 model across several shallow and deep peat deposits in Manitoba, Canada.

775 **4.1.2. Hypothesis 2: Increase in GPP with WTD drawdown**

776 WTD variations affected GPP in *ecosys* by affecting root and microbial O₂ availability,
777 energy yields, root and microbial growth and decomposition, rates of mineralization and hence
778 root nutrient availability and uptake. Wet soils under shallow WT caused low O₂ diffusion (Fig.
779 4c) (Eqs. D42-D44) into the peat and consequent low [O_{2s}] meant that root O₂ demand had to be
780 mostly met by [O_{2r}]. *Ecosys* inputs for root porosity ($\theta_{pr}=0.1$) that governed O₂ transport
781 through aerenchyma (Eq. D45) and hence maintained [O_{2r}] was not enough to meet the root O₂
782 demand in saturated soil by the two over-storey tree PFTs i.e. black spruce and tamarack,
783 causing shallow root systems to be simulated in these two tree PFTs under shallow WTD (Sect.
784 3.4). The under-storey shrub PFT (dwarf birch) had a higher root porosity ($\theta_{pr}=0.3$) and hence
785 had deeper rooting under shallow WT than the two tree PFTs (Sect. 3.4). Shallow rooting in the
786 tree PFTs reduced root surface area for nutrient uptake. Root nutrient uptake (Eqs. C23b, d, f) in
787 all the PFTs was also constrained by low nutrient availability due to smaller aqueous
788 concentrations of NH₄⁺, NO₃⁻ and/or H₂PO₄⁻ (Eqs. C23a, c, e) resulting from slower
789 mineralization (Eq. A26) of DON and DOP (Eq. A7) because of low [O_{2s}] in the wet soils under
790 shallow WT. Slower root growth and nutrient uptake caused lower foliar σ_N and/or σ_P with
791 respect to foliar σ_C (Eq. C11) that slowed the rates of carboxylation (Eq. C6) and hence reduced
792 vascular GPP (Eq. C1) under shallow WT.



793 WTD drawdown enhanced O_2 diffusion (Fig. 4c) (Eqs. D42-D44) and raised $[O_{2s}]$ so that
794 root O_2 demand in all the three vascular PFTs was almost entirely met by $[O_{2s}]$. Consequently
795 roots in all the PFTs could grow deeper which increased the root surface for nutrient uptake
796 (Sect. 3.4). Increase in modelled root growth due to WTD drawdown could be corroborated by
797 the increase in maximum rooting depth in black spruce and tamarack from 0.2-0.3 to 0.6 m with
798 a WTD drawdown from 0.14 to 0.9 m as a result of artificial drainage in a similar fen peatland in
799 Central Alberta as measured by Lieffers and Rothwell (1987). Murphy et al. (2009) also found a
800 significant increase in tree fine root production with WTD drawdown from ~0.1 to ~0.25 m
801 during a WTD manipulation study in a Finish peatland. Beside improved root growth, greater
802 $[O_{2s}]$ under deeper WT also enhanced rates of mineralization (Eq. A26) of DON and DOP (Eq.
803 A7) that raised aqueous concentrations of NH_4^+ , NO_3^- and/or $H_2PO_4^-$ and hence facilitated root
804 nutrient availability and uptake. Enhanced root nutrient uptake increased foliar σ_N and/or σ_P with
805 respect to foliar σ_C (Eq. C11) that hastened the rates of carboxylation (Eq. C6) and hence raised
806 vascular GPP (Eq. C1) under deeper WT.

807 The three modelled vascular PFT were predominantly N limited as indicated by mass-
808 based modelled foliar N to P ratios of 6.6:1, 5.2:1 and 4.8:1 for black spruce, tamarack and dwarf
809 birch under shallow WT in the growing season of 2004. Modelled N to P ratios were
810 corroborated by mass-based foliar N to P ratios of 7.1:1 and 6.3:1 for black spruce and tamarack
811 measured by Syed et al. (2006) at our site during the summer of 2004. Mass-based foliar N to P
812 ratio less than 16:1 usually indicates that the particular vegetation is more N than P limited
813 (Aerts and Chapin III, 1999). Since the modelled PFTs were predominantly N limited, increases
814 in foliar N concentrations as a result of improved root nutrient availability, growth and nutrient
815 uptake with WTD drawdown enhanced modelled carboxylation rates and hence modelled GPP.



816 Choi et al. (2007) in a WT manipulation study found an increase in peat NO_3^- -N due to enhanced
817 mineralization and nitrification stimulated by a WTD drawdown from 0.24 to 0.7 m below the
818 surface that caused increases in foliar N concentrations from ~ 21 to $\sim 27 \text{ g kg}^{-1} \text{ C}$ (assuming 50%
819 of dry matter as organic C) in black spruce and ~ 41 to $\sim 66 \text{ g kg}^{-1} \text{ C}$ in tamarack in a Central
820 Albertan fen peatland. Increases in foliar N concentrations due to enhanced root nutrient
821 availability and uptake with WTD drawdown in their study also caused significantly greater
822 radial tree growth. Macdonald and Lieffers (1990) in a WTD manipulation study also found that
823 WTD drawdown by $\sim 0.45 \text{ m}$ raised foliar N concentrations from ~ 19 to $\sim 21 \text{ g kg}^{-1} \text{ C}$ (assuming
824 50% of dry matter as organic C) in black spruce and ~ 36 to $\sim 42 \text{ g kg}^{-1} \text{ C}$ in tamarack trees that
825 enhanced net photosynthetic C assimilation rates by those tree species in an Albertan moderately
826 rich fen. The rates of increases in foliar N concentrations in black spruce and tamarack trees due
827 to WTD drawdown in similar peatlands are comparable with those in our modelled outputs (Sect.
828 3.4).

829 Modelled growing season GPP increased by $0.39 \mu\text{mol CO}_2 \text{ m}^{-2} \text{ s}^{-1}$ per 0.1 m WTD
830 drawdown which was greater than the EC-derived GPP increase of $0.22 \mu\text{mol CO}_2 \text{ m}^{-2} \text{ s}^{-1}$ per 0.1
831 m WTD drawdown as reported by Flanagan and Syed (2011) for the WPL over the growing
832 seasons of 2004-2009. However, the modelled GPP increase with WTD drawdown was
833 comparable with the range of 0.28 to $0.4 \mu\text{mol CO}_2 \text{ m}^{-2} \text{ s}^{-1}$ per 0.1 m WTD drawdown reported
834 by Peichl et al. (2014) and Ballantyne et al. (2014) for northern boreal fen peatlands in Michigan
835 and Sweden.



836 **4.1.3. Hypothesis 3: Microbial water stress on R_e due to WT deepening below a threshold**

837 **WTD**

838 When WT in *ecosys* dropped below a threshold level of ~0.3 m from the hollow surface
839 (~0.6 m below the hummock surface), near surface peat desiccation reduced microbial access to
840 substrate for decomposition (Eq. A15) which enabled *ecosys* to simulate reduction in near
841 surface R_h . When reduction in near surface R_h more than fully offset the increase in deeper R_h ,
842 net ecosystem R_h decreased. The offsetting effect on R_h partly contributed to simulated decrease
843 in growing season R_e ($=R_h+R_a$) from 2008 to 2009 with WTD drawdown that was corroborated
844 by a similar decrease in EC-derived R_e (Fig. 6c). Greater reductions in R_h in desiccated near
845 surface peat layers also caused the reductions in growing season R_e in drainage cycle 2 from
846 those in cycle 1 during 2007-2009 in the simulated drainage study (Fig. 8d). Similar to our study,
847 Peichl et al. (2014) found reductions in R_e when WTD fell below a threshold of ~0.3 m from the
848 peat surface in a Swedish fen which could be partially attributed to reduction in near surface R_h
849 due to desiccation. Mettrop et al. (2014) in a controlled incubation experiment found that the
850 rates of microbial respiration in a nutrient rich Dutch fen initially increased with peat drying and
851 consequent improved aeration. But excessive drying and consequent peat desiccation in their
852 study reduced microbial respiration efficiency, growth and biomass. Dimitrov et al. (2010a) in a
853 modelling study using *ecosys* also showed that a decrease in desiccated near surface peat
854 respiration partially offset increased deeper peat respiration when WT deepened below a
855 threshold of ~0.6-0.7 m from the hummock surface.



856 **4.1.4. Hypothesis 4: Plant water stress on GPP due to WT deepening below a threshold**

857 **WTD**

858 Deepening of WT below a threshold level also caused rapid peat pore drainage and low
859 moisture contents in the near surface peat layers which were colonized by most of the vascular
860 root systems and all of the non-vascular mosses (Eqs. D9-D29). When WTD fell below ~ 0.1 m
861 from the hollow surface (~ 0.4 m below the hummock surface), vertical recharge through
862 capillary rise from the WT was not adequate to maintain near surface peat moisture. It reduced
863 peat water potential (ψ_s) and raised peat hydraulic resistance (Ω_s) (Eq. B9) that suppressed root
864 and moss water uptake (U_w) (Eq. B6) from desiccated near surface peat layers. Since moss U_w
865 entirely depended upon moisture supply from the near surface layers, reduction in U_w from
866 desiccation of these layers caused reduction in moss canopy water potential (ψ_c) (Mezbahuddin
867 et al., 2016) and hence moss GPP (Eqs. C1, C4). Reduction in root U_w from desiccated near
868 surface layers, however, was offset by increased root U_w (Eq. B6) from deeper wetter layers,
869 which had higher ψ_s and lower Ω_s , due to deeper root growth facilitated by enhanced aeration. It
870 enabled the vascular PFTs in *ecosys* to sustain ψ_c , canopy turgor potential (ψ_t) (Eq. B4), stomatal
871 conductance (g_c) (Mezbahuddin et al., 2016) (Eqs. B2, C4) and hence to sustain increased GPP
872 (Eq. C1) due to higher root nutrient availability and uptake. Increased vascular GPP and
873 consequent greater vascular plant growth further imposed limitations of water, nutrient and light
874 to the modelled non-vascular PFTs due to interspecific competition and greater shading from the
875 overstorey vascular PFTs. However, increases in vascular GPP due to enhanced plant nutrient
876 status more than fully offset the suppression in moss GPP due to moss drying, and greater
877 shading and competition from the overstorey, thereby causing a net increase in modelled GPP
878 with WTD drawdown (Figs. 6b and 9b-c). This modelled trend indicated increased vascular



879 dominance over moss with deepening of WT in the model. Several WTD manipulation studies
880 (e.g., Moore et al., 2006, Munir et al., 2014) in similar northern boreal peatlands reported
881 increased tree, shrub and herb growths over mosses with WTD drawdown that corroborates our
882 modelled trend. Gains in modelled vascular GPP halted and eventually vascular GPP started to
883 decline when WT fell below ~ 0.6 m from the hollow surface (~ 0.9 m below the hummock
884 surface) in our drainage simulation (Figs. 9c, e). It was because deeper root U_w (Eq. B6) could no
885 longer offset suppression of near-surface root U_w when WT fell below threshold WTD, thereby
886 causing lower ψ_c , ψ_A (Eq. B4), g_c (Eqs. B2, C4) and slower CO_2 fixation (Eq. C6).

887 Similar to our modelling study, Riutta et al. (2007) measured a reduction in moss
888 productivity due to water limitation when WTD fell below ~ 0.15 m from the surface in a Finish
889 fen peatland. However, vascular GPP during that period sustained in their study indicating no
890 vascular water stress (Riutta et al., 2007). Peichl et al. (2014) measured reduction in moss GPP
891 due to moss drying when WTD fell below ~ 0.3 m from the surface in a Swedish fen. They
892 inferred that the peat in their study did not have sufficient moisture supplying capacity through
893 capillary rise to sustain moss U_w when the WT fell below ~ 0.3 m from the surface. Reductions in
894 moss GPP due to decreased moss canopy water potentials were also modelled by Dimitrov et al.
895 (2011) using the same model *ecosys* when WTD fell below ~ 0.3 m from the hummock surface of
896 a Canadian bog. They, however, found no vascular plant water stress and hence no reduction in
897 vascular GPP during that period. Similarly, Kuiper et al. (2014) found reductions in moss
898 productivity with peat drying while vascular productivity sustained in a simulated drought
899 experiment on a Danish peat.

900 Continued deepening of WT can also cause vascular plant water stress and hence
901 reductions in vascular GPP as modelled in our study (Figs. 9c, e). It can also be corroborated by



902 field measurements across various northern boreal fen peatlands in Canada and Sweden.
903 Sonnentag et al. (2010) found a reduction in canopy stomatal conductance (g_c) and hence
904 vascular GPP when WT fell below ~ 0.4 m from the ridge surface at a fen peatland in
905 Saskatchewan. The dominant vascular vegetation in their study included tamarack and dwarf
906 birch, two of the three vascular PFTs in our modelling thereby further corroborating the
907 projected vascular water stress. Peichl et al. (2014) also found a reduction in vascular GPP due to
908 plant water stress when WTD fell below ~ 0.3 m from the surface in a Swedish fen peatland. The
909 WTD threshold for reductions in vascular GPP in those two field studies were shallower than
910 that in our modelled projection i.e. ~ 0.6 m from the hollow surface (~ 0.9 m below the hummock
911 surface) (Figs. 9a, c, e) thereby indicating different vertical rooting patterns determined by
912 specific interactions between hydrologic properties and rooting. Lafleur et al. (2005) and
913 Schwärzel et al. (2006) found much deeper WTD thresholds for reductions in vascular
914 transpiration that could negatively affect vascular GPP over a Canadian pristine peatland and a
915 German drained peatland. Those WTD thresholds were ~ 0.65 and ~ 0.9 m below the surface for
916 pristine and drained peatland respectively, further indicating the importance of root-hydrology
917 interactions and the resultant root adaptations, growth and uptake in determining WTD effects on
918 vascular GPP across peatlands.

919 **4.2. Divergences between modelled and EC-derived annual GPP, R_e and NEP**

920 Modelled annual GPP and R_e were consistently larger than EC-derived estimates of GPP
921 and R_e during 2005-2008 (Figs. 6f-g). Despite larger modelled vs. EC-derived GPP and R_e ,
922 modelled annual NEP was consistently lower than the EC gap-filled annual NEP (Fig. 6e).
923 Smaller modelled NEP estimates were caused by larger modelled vs. EC-derived R_e than
924 modelled vs. EC-derived GPP (Figs. 6f-g). Larger deviation between modelled and EC-derived



925 R_e estimates was mainly contributed by gap filled night-time CO_2 fluxes ($=R_e$) which was also
926 apparent in negative intercepts from modelled on gap-filled net CO_2 flux regressions (Table 1).
927 The gap-filling for night-time CO_2 fluxes was done by Syed et al. (2006) using empirical
928 relationships between EC CO_2 measurements and soil temperature (T_s) measured at 0.05 m depth
929 at the WPL. During night-time and the winter, peat at this shallow depth (0.05 m) could have
930 rapidly cooled down and thus yielded smaller night-time gap-filled CO_2 fluxes (Figs. 2, 4 and 5).
931 On the contrary, modelled CO_2 fluxes in those periods depended on the temperatures of not only
932 the shallow peat layers but also the deeper peat profiles that were warmer than the shallower
933 layers and hence simulated larger CO_2 effluxes than the gap-filled (e.g., Figs. 4a, 5h-i). CO_2
934 fluxes measured by automated chamber in cooler nights, however, did not decline as rapidly as
935 did the gap-filled CO_2 fluxes as night progressed further corroborating this reasoning for larger
936 modelled vs. gap-filled R_e during night-time and the winter (e.g., Figs. 4b vs. 4a, 5j-k vs. 5h-i).

937 Systematic uncertainties embedded in EC methodology could also contribute to larger
938 modelled vs. EC-derived annual and growing season R_e estimates (Figs. 6c, g). The major
939 uncertainty in the EC methodology is the possible underestimation of nighttime EC CO_2 flux
940 measurements due to poor turbulent mixing under stable air conditions (Goulden et al., 1997;
941 Miller et al., 2004). On the contrary, modelled biological production of CO_2 by plant and
942 microbial respiration was independent of turbulent mixing which would thus contribute to larger
943 modelled than EC-derived R_e estimates.

944 Larger modelled vs. gap-filled R_e might have also contributed to larger modelled vs. gap-
945 filled growing season and annual GPP (Figs. 6b, f). In EC datasets, GPP was derived from R_e .
946 Smaller gap-filled vs. modelled R_e would thus cause smaller EC-derived vs. modelled GPP.
947 Complete energy balance closure in the model vs. incomplete (~75%) energy balance closure in



948 EC measurements would also cause a larger modelled than measured evapotranspiration
949 (Mezbahuddin et al., 2016) and possibly GPP (Figs. 6b, f). Unlike decoupled GPP and R_e during
950 gap-filling, modelled GPP influenced modelled R_e through root exudation and litter fall which
951 further contributed to deviation between modelled vs. EC-derived growing season and annual R_e
952 estimates (Figs. 6c, g). So, the uncertainties in the modelling that arose from discrepancies
953 between modelled and EC-derived R_e and GPP aggregates could not be resolved without
954 resolving the above mentioned uncertainties in EC methodology, and gap-filling, and
955 partitioning of EC-gap filled NEP into GPP and R_e .

956 5. Conclusions

957 Coupling of eco-hydrology and biogeochemistry algorithms in *ecosys* simulated increases
958 in R_e and GPP with deepening of WT from 2004 to 2009 in the boreal fen at the WPL. Similar
959 increases in R_e and GPP, however, left no net effect of WT deepening on modelled variations in
960 NEP. This modelled trend was corroborated by EC-derived NEP, R_e and GPP (Syed et al., 2006;
961 Flanagan and Syed, 2011) and automated chamber measured NEP and R_e (Cai et al., 2010) at the
962 WPL. The effects of WTD drawdown on R_e and GPP was modelled in *ecosys* by the algorithms
963 representing following processes:

964 (1) Improved $[O_{2s}]$ facilitated by rapid O_2 diffusion (Eqs. D42-D44) under deeper WT raised
965 microbial energy yields while oxidizing DOC coupled with O_2 reduction (Eq. A21) and
966 hence caused increases in R_e . Increased mineralization rates of DON and DOP due to
967 improved $[O_{2s}]$ also increased aqueous concentrations of NH_4^+ , NO_3^- and $H_2PO_4^-$ (Eqs.
968 C23a, c, e) that facilitated microbial nutrient availability, uptake (Eq. A22) and growth
969 (Eq. A29) and hence further enhanced R_e .



- 970 (2) Increased nutrient availability due to rapid mineralization with WTD drawdown as
971 mentioned above hastened root nutrient (mainly N) availability and uptake (Eqs. C23b, d,
972 f). Root nutrient availability and uptake in *ecosys* were further facilitated by increased
973 root growth stimulated by improved $[O_{2s}]$ under deeper WT. Greater root growth and
974 uptake thus caused improved foliar σ_N with respect to σ_C thereby enhancing CO_2 fixation
975 (Eq. C6) and vascular GPP (Eq. C1).
- 976 (3) When WT in *ecosys* dropped below ~ 0.3 m from the hollow surface (~ 0.6 m below the
977 hummock surface), inadequate capillary recharge from WT caused desiccation of near
978 surface peat layers and surface residues (Eqs. D9, D12). Surface and near surface peat
979 desiccation raised microbial concentrations and reduced microbial access to substrate for
980 decomposition in these desiccated layers (Eq. A15). It enabled *ecosys* to simulate
981 reduction in R_h in the desiccated peats from competitive inhibition of microbial exo-
982 enzymes with increasing concentrations (Figs. 6c, 8d) (Eq. A4).
- 983 (4) When WT fell below ~ 0.1 m from the hollow surface (~ 0.4 m below the hummock
984 surface) vertical recharge of near surface peat layers through capillary rise from WT was
985 not enough to sustain moss water uptake thereby causing moss drying and consequent
986 reduced moss GPP (Eqs. C1, C4). However, sustained increases in vascular GPP due to
987 root water uptake from deeper wetter layers more than fully offset the suppression of
988 moss GPP thereby causing a net increase in GPP with WTD drawdown (Figs. 6b and 9b-
989 c).
- 990 These modelling hypotheses were also corroborated by various field, laboratory and modelling
991 studies over similar peatlands (Sect. 4.1). Moreover, the projected drainage simulation showed
992 that the increase in vascular GPP due to improved plant nutrient status caused by WTD



993 drawdown would only sustain while WTD remained above a threshold level i.e. ~ 0.6 m below
994 the hollow surface (~ 0.9 m below the hummock surface). When WT fell below this threshold,
995 projected vascular GPP started to decrease with further WTD drawdown thereby causing
996 reductions in ecosystem GPP. Similar WTD threshold effects on vascular GPP were also found
997 in other studies in similar peatlands (Sect. 4.1.2).

998 Therefore, representing feedbacks between peatland hydrological and C processes in
999 *ecosys* enabled successful simulation of WTD effects on R_e , GPP and hence NEP of a northern
1000 boreal fen peatland. Projected drainage simulation in our study showed that continued WTD
1001 could alter ecosystem C balance of northern boreal peatlands by decreasing GPP and sustaining
1002 increased R_e thereby causing declines in NEP. These findings provide us with important insights
1003 into how northern boreal peatland C stocks would be affected by likely WTD drawdown under
1004 future drier and warmer climates. This study is also reproducible in other peatlands when the
1005 model is fed by required physical, hydrological, chemical, biological and ecological inputs those
1006 are measurable at the sites (Fig. 1) (Mezbahuddin et al., 2016). Successful simulation of
1007 hydrological effects on peatland C processes by *ecosys* for a northern boreal fen peatland in this
1008 study along with simulations of feedbacks between hydrology, biogeochemistry and ecology by
1009 the same model *ecosys* across other contrasting peatlands (e.g., Dimitrov et al., 2011; Grant et
1010 al., 2012; Mezbahuddin et al., 2014, 2015, 2016) would, therefore, provide us with a modelling
1011 framework for large scale (e.g., regional/continental/global) peatland C simulations, which
1012 currently is one of the most sought after in global terrestrial ecosystem carbon modelling
1013 community.



1014 **Code availability**

1015 The *ecosys* model codes are listed in equation forms and sufficiently described in the
1016 supplementary material. The model codes that were written in FORTRAN will also be available
1017 on request from either symon.mezbahuddin@gov.ab.ca or rgrant@ualberta.ca.



1018 **Data availability**

1019 Field data that were used to validate model outputs are available at

1020 <http://fluxnet.ornl.gov/site/292>.



1021 **Author contribution**

1022 M. Mezbahuddin contributed to the model code modification and development, designing
1023 modelling experiment, simulation, validation, and analyses of modelled outputs. R. F. Grant is
1024 the original developer of the model *ecosys* and also contributed into simulation design and model
1025 runs. L. B. Flanagan was site principal investigator who led the collection, and quality control of
1026 the field data that were used to validate model outputs. M. Mezbahuddin wrote the manuscript
1027 with significant contributions from R. F. Grant and L. B. Flanagan.



1028 **Acknowledgments**

1029 Computing facilities for the modelling project was provided by Compute Canada,
1030 Westgrid, and University of Alberta. Funding for the modelling project was provided by several
1031 research awards from Faculty of Graduate Studies and Research and Department of Renewable
1032 Resources of University of Alberta and a Natural Sciences and Engineering Research Council
1033 (NSERC) of Canada discovery grant. The field research was carried out as part of the Fluxnet-
1034 Canada Research Network and the Canadian Carbon Program and was funded by grants to
1035 Lawrence B. Flanagan from NSERC, Canadian Foundation for Climate and Atmospheric
1036 Sciences, and BIOCAP Canada.



1037 **References**

- 1038 Aerts, R. and Chapin III, F.: The mineral nutrition of wild plants revisited: a re-evaluation of
1039 processes and patterns, *Adv. Ecol. Res.*, 30, 1-67, doi:10.1016/S0065-2504(08)60016-1,
1040 1999.
- 1041 Baker, I. T., Prihodko, L., Denning, A. S., Goulden, M., Miller, S., and Da Rocha, H. R.:
1042 Seasonal drought stress in the Amazon: reconciling models and observations, *J. Geophys.*
1043 *Res.-Biogeo.*, 113, G00B01, doi:10.1029/2007JG000644, 2008.
- 1044 Ballantyne, D. M., Hribljan, J. A., Pypker, T. G., and Chimner, R. A.: Long-term water table
1045 manipulations alter peatland gaseous carbon fluxes in Northern Michigan, *Wetl. Ecol.*
1046 *Manag.*, 22, 35-47, doi:10.1007/s11273-013-9320-8, 2014.
- 1047 Bond-Lamberty, B., Gower, S. T., and Ahl, D. E.: Improved simulation of poorly drained forests
1048 using Biome-BGC, *Tree Physiol.*, 27, 703-715, doi:10.1093/treephys/27.5.703, 2007.
- 1049 Cai, T., Flanagan, L. B., and Syed, K. H.: Warmer and drier conditions stimulate respiration
1050 more than photosynthesis in a boreal peatland ecosystem: analysis of automatic chambers
1051 and eddy covariance measurements, *Plant Cell Environ.*, 33, 394-407, doi:10.1111/j.1365-
1052 3040.2009.02089.x, 2010.
- 1053 Campbell, G. S.: A simple method for determining unsaturated conductivity from moisture
1054 retention data, *Soil Sci.*, 117, 311-314, 1974.
- 1055 Choi, W. J., Chang, S. X., and Bhatti, J. S.: Drainage affects tree growth and C and N dynamics
1056 in a minerotrophic peatland, *Ecology*, 88, 443-453, doi:10.1890/0012-
1057 9658(2007)88[443:DATGAC]2.0.CO;2, 2007.



- 1058 Cronk, J. K. and Fennessy, M. S.: Wetland plants: biology and ecology, CRC press, 2001.
- 1059 Dimitrov, D. D., Grant, R. F., Lafleur, P. M., and Humphreys, E. R.: Modeling the effects of
1060 hydrology on ecosystem respiration at Mer Bleue bog, *J. Geophys. Res.-Biogeo.*, 115,
1061 G04043, doi:10.1029/2010JG001312, 2010a.
- 1062 Dimitrov, D. D., Grant, R. F., Lafleur, P. M., and Humphreys, E. R.: Modelling subsurface
1063 hydrology of Mer Bleue bog, *Soil Sci. Soc. Am. J.*, 74, 680–694,
1064 doi:10.2136/sssaj2009.0148, 2010b.
- 1065 Dimitrov, D. D., Grant, R. F., Lafleur, P. M., and Humphreys, E. R.: Modeling the effects of
1066 hydrology on gross primary productivity and net ecosystem productivity at Mer Bleue bog,
1067 *J. Geophys. Res.-Biogeo.*, 116, G04010, doi:10.1029/2010JG001586, 2011.
- 1068 Dise, N. B: Peatland response to global change, *Science*, 326, 810-811,
1069 doi:10.1126/science.1174268, 2009.
- 1070 Flanagan, L. B. and Syed, K. H.: Stimulation of both photosynthesis and respiration in response
1071 to warmer and drier conditions in a boreal peatland ecosystem, *Glob. Change Biol.*, 17,
1072 2271-2287, doi:10.1111/j.1365-2486.2010.02378.x, 2011.
- 1073 Frohling, S., Roulet, N. T., Moore, T. R., Lafleur, P. M., Bubier, J. L., and Crill, P. M.:
1074 Modelling the seasonal to annual carbon balance of Mer Bleue bog, Ontario, Canada,
1075 *Global Biogeochem. Cy.*, 16, 1-21, doi:10.1029/2001GB001457, 2002.
- 1076 Gerten, D., Schaphoff, S., Haberlandt, U., Lucht, W., and Sitch, S.: Terrestrial vegetation and
1077 water balance-hydrological evaluation of a dynamic global vegetation model, *J. Hydrol.*,
1078 286, 249-270, doi:10.1016/j.jhydrol.2003.09.029, 2004.



- 1079 Gorham, E: Northern peatlands: role in the carbon cycle and probable responses to climatic
1080 warming, *Ecol. Appl.*, 1, 182-195, doi: 10.2307/1941811, 1991.
- 1081 Goulden, M. L., Daube, B. C., Fan, S. M., Sutton, D. J., Bazzaz, A., Munger, J. W., and Wofsy,
1082 S. C.: Physiological responses of a black spruce forest to weather, *J. Geophys. Res.-*
1083 *Atmos.*, 102, 28987-28996, doi:10.1029/97JD01111, 1997.
- 1084 Grant, R. F., Desai, A. R., and Sulman, B. N.: Modelling contrasting responses of wetland
1085 productivity to changes in water table depth, *Biogeosciences*, 9, 4215-4231,
1086 doi:10.5194/bg-9-4215-2012, 2012.
- 1087 Ise, T., Dunn, A. L., Wofsy, S. C., and Moorcroft, P. R.: High sensitivity of peat decomposition
1088 to climate change through water-table feedback, *Nat. Geosci.*, 1, 763-766,
1089 doi:10.1038/ngeo331, 2008.
- 1090 Kotowska, A: The long-term effects of drainage on carbon cycling in a boreal fen, M.Sc. thesis,
1091 Department of Integrative Biology, University of Guelph, Ontario, Canada, 75 pp., 2013.
- 1092 Krinner, G., Viovy, N., de Noblet-Ducoudré, N., Ogée, J., Polcher, J., Friedlingstein, P., Ciais,
1093 P., Sitch, S., and Prentice, I. C.: A dynamic global vegetation model for studies of the
1094 coupled atmosphere-biosphere system, *Global Biogeochem. Cy.*, 19, GB1015,
1095 doi:10.1029/2003GB002199, 2005.
- 1096 Kuiper, J. J., Mooij, W. M., Bragazza, L., and Robroek, B. J.: Plant functional types define
1097 magnitude of drought response in peatland CO₂ exchange, *Ecology*, 95, 123-131,
1098 doi:10.1890/13-0270.1, 2014.



- 1099 Lafleur, P. M., Moore, T. R., Roulet, N. T., and Frohling, S.: Ecosystem respiration in a cool
1100 temperate bog depends on peat temperature but not on water table, *Ecosystems*, 8, 619-
1101 629, doi:10.1007/s10021-003-0131-2, 2005.
- 1102 Lieffers, V. J. and Rothwell, R. L.: Rooting of peatland black spruce and tamarack in relation to
1103 depth of water table, *Can. J. Botany*, 65, 817-821, doi: 10.1139/b87-111, 1987.
- 1104 Limpens, J., Berendse, F., Blodau, C., Canadell, J. G., Freeman, C., Holden, J., Roulet, N.,
1105 Rydin, H., and Schaepman-Strub, G.: Peatlands and the carbon cycle: from local processes
1106 to global implications – a synthesis, *Biogeosciences*, 5, 1475–1491, doi:10.5194/bg-5-
1107 1475-2008, 2008.
- 1108 Lizama, H. M. and Suzuki, I.: Kinetics of sulfur and pyrite oxidation by *Thiobacillus*
1109 thiooxidans. Competitive inhibition by increasing concentrations of cells, *Can. J.*
1110 *Microbiol.*, 37, 182-187, doi:10.1139/m91-028, 1991.
- 1111 Long, K. D., Flanagan, L. B., and Cai, T.: Diurnal and seasonal variation in methane emissions
1112 in a northern Canadian peatland measured by eddy covariance, *Glob. Change Biol.* 16,
1113 2420-2435, doi:10.1111/j.1365-2486.2009.02083.x, 2010.
- 1114 Long, K. D.: Methane fluxes from a northern peatland: mechanisms controlling diurnal and
1115 seasonal variation and the magnitude of aerobic methanogenesis, M.Sc. thesis, Department
1116 of Biological Sciences, University of Lethbridge, Lethbridge, AB, Canada, 100 pp., 2008.
- 1117 Macdonald, S. E. and Lieffers, V. J.: Photosynthesis, water relations, and foliar nitrogen of *Picea*
1118 *mariana* and *Larix laricina* from drained and undrained peatlands, *Can. J. Forest Res.*, 20,
1119 995-1000, doi:10.1139/x90-133, 1990.



- 1120 Mäkiranta, P., Laiho, R., Fritze, H., Hytönen, J., Laine, J., and Minkkinen, K.: Indirect regulation
1121 of heterotrophic peat soil respiration by water level via microbial community structure and
1122 temperature sensitivity, *Soil Biol. Biochem.*, 41, 695-703,
1123 doi:10.1016/j.soilbio.2009.01.004, 2009.
- 1124 Markham, J. H.: Variation in moss-associated nitrogen fixation in boreal forest stands, *Oecologia*
1125 161, 353-359, doi: 10.1007/s00442-009-1391-0, 2009.
- 1126 Mettrop, I. S., Cusell, C., Kooijman, A. M., and Lamers, L. P.: Nutrient and carbon dynamics in
1127 peat from rich fens and Sphagnum-fens during different gradations of drought, *Soil Biol.*
1128 *Biochem.*, 68, 317-328, doi:10.1016/j.soilbio.2013.10.023, 2014.
- 1129 Mezbahuddin, M., Grant, R. F., and Hirano, T.: How hydrology determines seasonal and
1130 interannual variations in water table depth, surface energy exchange, and water stress in a
1131 tropical peatland: modeling versus measurements, *J. Geophys. Res.-Biogeo.*, 120, 2132-
1132 2157, doi:10.1002/2015JG003005, 2015.
- 1133 Mezbahuddin, M., Grant, R. F., and Hirano, T.: Modelling effects of seasonal variation in water
1134 table depth on net ecosystem CO₂ exchange of a tropical peatland, *Biogeosciences*, 11,
1135 577-599, doi:10.5194/bg-11-577-2014, 2014.
- 1136 Mezbahuddin, M., Grant, R.F. and Flanagan, L.B.: Modeling hydrological controls on variations
1137 in peat water content, water table depth, and surface energy exchange of a boreal western
1138 Canadian fen peatland, *J. Geophys. Res.-Biogeo.*, 121, 2216-2242,
1139 doi:10.1002/2016JG003501, 2016.



- 1140 Miller, S. D., Goulden, M. L., Menton, M. C., da Rocha, H. R., de Freitas, H. C., Figueira, A. M.
1141 e. S., and de Sousa, C. A. D.: Biometric and micrometeorological measurements of tropical
1142 forest carbon balance, *Ecol. Appl.*, 14, 114–126, doi:10.1890/02-6005, 2004.
- 1143 Moore, T. and Basiliko, N.: Decomposition in boreal peatlands, in: *Boreal peatland ecosystems*,
1144 edited by: Wieder, R. K. and Vitt, D. H., Springer Science & Business Media, 125-143,
1145 2006.
- 1146 Munir, T. M., Xu, B., Perkins, M., and Strack, M.: Responses of carbon dioxide flux and plant
1147 biomass to water table drawdown in a treed peatland in northern Alberta: a climate change
1148 perspective, *Biogeosciences*, 11, 807-820, doi:10.5194/bg-11-807-2014, 2014.
- 1149 Murphy, M., Laiho, R., and Moore, T. R.: Effects of water table drawdown on root production
1150 and aboveground biomass in a boreal bog, *Ecosystems*, 12, 1268-1282,
1151 doi:10.1007/s10021-009-9283-z, 2009.
- 1152 Parmentier, F. J. W., Van der Molen, M. K., de Jeu, R. A. M., Hendriks, D. M. D., and Dolman,
1153 A. J.: CO₂ fluxes and evaporation on a peatland in the Netherlands appear not affected by
1154 water table fluctuations, *Agr. Forest Meteorol.*, 149, 1201-1208,
1155 doi:10.1016/j.agrformet.2008.11.007, 2009.
- 1156 Peichl, M., Öquist, M., Löfvenius, M. O., Ilstedt, U., Sagerfors, J., Grelle, A., Lindroth, A., and
1157 Nilsson, M. B.: A 12-year record reveals pre-growing season temperature and water table
1158 level threshold effects on the net carbon dioxide exchange in a boreal fen, *Environ. Res.
1159 Lett.*, 9, 055006, doi:10.1088/1748-9326/9/5/055006, 2014.



- 1160 Preston, M. D., Smemo, K. A., McLaughlin, J. W., and Basiliko, N.: Peatland microbial
1161 communities and decomposition processes in the James Bay Lowlands, Canada, *Front.*
1162 *Microbiol.*, 3, 70, doi:10.3389/fmicb.2012.00070, 2012.
- 1163 Richardson, A. D., Hollinger, D. Y., Burba, G. G., Davis, K. J., Flanagan, L. B., Katul, G. G.,
1164 Munger, J. W., Ricciuto, D. M., Stoy, P. C., Suyker, A. E., Verma, S. B., and Wofsy, S. C.:
1165 A multi-site analysis of random error in tower-based measurements of carbon and energy
1166 fluxes, *Agr. Forest Meteorol.*, 136, 1-18, doi:10.1016/j.agrformet.2006.01.007, 2006.
- 1167 Rippy, J. F. and Nelson, P. V.: Cation exchange capacity and base saturation variation among
1168 Alberta, Canada, moss peats, *HortScience*, 42, 349-352, 2007.
- 1169 Riutta, T., Laine, J., and Tuittila, E. S.: Sensitivity of CO₂ exchange of fen ecosystem
1170 components to water level variation, *Ecosystems*, 10, 718-733, doi:10.1007/s10021-007-
1171 9046-7, 2007.
- 1172 Riutta, T.: Fen ecosystem carbon gas dynamics in changing hydrological conditions, *Diss. For.*
1173 67, Department of Forest Ecology, Faculty of Agriculture and Forestry, University of
1174 Helsinki, 46pp., 2008.
- 1175 Schaefer, K., Collatz, G. J., Tans, P., Denning, A. S., Baker, I., Berry, J., Prihodko, L., Suits, N.,
1176 and Philpott, A.: Combined simple biosphere/Carnegie-Ames-Stanford approach terrestrial
1177 carbon cycle model, *J. Geophys. Res.-Biogeo.*, 113, G03034, doi:10.1029/2007JG000603,
1178 2008.



- 1179 Schwärzel, K., Šimunek, J., van Genuchten, M. T., and Wessolek, G.: Measurement and
1180 modeling of soil-water dynamics and evapotranspiration of drained peatland soils, *J. Plant*
1181 *Nutr. Soil Sci.*, 169, 762-774, doi:10.1002/jpln.200621992, 2006.
- 1182 Sonnentag, O., van der Kamp, G., Barr, A. G., and Chen, J. M.: On the relationship between
1183 water table depth and water vapour and carbon dioxide fluxes in a minerotrophic fen, *Glob.*
1184 *Change Biol.*, 16, 1762–1776, doi:10.1111/j.1365-2486.2009.02032.x, 2010.
- 1185 St-Hilaire, F., Wu, J., Roulet, N. T., Frohling, S., Lafleur, P. M., Humphreys, E. R., and Arora,
1186 V.: McGill wetland model: evaluation of a peatland carbon simulator developed for global
1187 assessments, *Biogeosciences*, 7, 3517–3530, doi:10.5194/bg-7-3517-2010, 2010.
- 1188 Strack, M., Waddington, J. M., Rochefort, L., and Tuittila, E. S.: Response of vegetation and net
1189 ecosystem carbon dioxide exchange at different peatland microforms following water table
1190 drawdown, *J. Geophys. Res.-Biogeo.*, 111, G02006, doi:10.1029/2005JG000145, 2006.
- 1191 Sulman, B. N., Desai, A. R., Cook, B. D., Saliendra, N., and Mackay, D. S.: Contrasting carbon
1192 dioxide fluxes between a drying shrub wetland in Northern Wisconsin, USA, and nearby
1193 forests, *Biogeosciences*, 6, 1115-1126, doi:10.5194/bg-6-1115-2009, 2009.
- 1194 Sulman, B. N., Desai, A. R., Saliendra, N. Z., Lafleur, P. M., Flanagan, L. B., Sonnentag, O.,
1195 Mackay, D. S., Barr, A. G., and van der Kamp, G.: CO₂ fluxes at northern fens and bogs
1196 have opposite responses to inter-annual fluctuations in water table, *Geophys. Res. Lett.*, 37,
1197 L19702, doi:10.1029/2010GL044018, 2010.
- 1198 Sulman, B. N., Desai, A. R., Schroeder, N. M., Ricciuto, D., Barr, A., Richardson, A. D.,
1199 Flanagan, L. B., Lafleur, P. M., Tian, H., Chen, G., Grant, R. F., Poulter, B., Verbeek, H.,



- 1200 Ciais, P., Ringeval, B., Baker, I. T., Schaefer, K., Luo, Y., and Weng, E.: Impact of
1201 hydrological variations on modeling of peatland CO₂ fluxes: Results from the North
1202 American Carbon Program site synthesis, *J. Geophys. Res.-Biogeo.*, 117, G01031,
1203 doi:10.1029/2011JG001862, 2012.
- 1204 Syed, K. H., Flanagan, L. B., Carlson, P. J., Glenn, A. J., and Van Gaalen, K. E.: Environmental
1205 control of net ecosystem CO₂ exchange in a treed, moderately rich fen in northern Alberta,
1206 *Agr. Forest Meteorol.*, 140, 97-114, doi:10.1016/j.agrformet.2006.03.022, 2006.
- 1207 Tian, H., Chen, G., Liu, M., Zhang, C., Sun, G., Lu, C., Xu, X., Ren, W., Pan, S., and Chappelka,
1208 A.: Model estimates of net primary productivity, evapotranspiration, and water use
1209 efficiency in the terrestrial ecosystems of the southern United States during 1895–2007,
1210 *Forest Ecol. Manag.*, 259, 1311-1327, doi:10.1016/j.foreco.2009.10.009, 2010.
- 1211 Turunen, J., Tomppo, E., Tolonen, K., and Reinikainen, A.: Estimating carbon accumulation
1212 rates of undrained mires in Finland-application to boreal and subarctic regions, *The*
1213 *Holocene*, 12, 69-80, 2002.
- 1214 Updegraff, K., Pastor, J., Bridgham, S. D., and Johnston, C. A.: Environmental and substrate
1215 controls over carbon and nitrogen mineralization in northern wetlands, *Ecol. Appl.*, 5, 151-
1216 163, doi:10.2307/1942060, 1995.
- 1217 van Genuchten, M. T.: A closed-form equation for predicting the hydraulic conductivity of
1218 unsaturated soils, *Soil Sci. Soc. Amer. J.*, 44, 892-898, doi:
1219 10.2136/sssaj1980.03615995004400050002x, 1980.



- 1220 Waddington, J. M., Morris, P. J., Kettridge, N., Granath, G., Thompson, D. K., and Moore, P. A.:
1221 Hydrological feedbacks in northern peatlands, *Ecohydrology*, 8, 113-127,
1222 doi:10.1002/eco.1493, 2015.
- 1223 Weng, E. and Luo, Y.: Soil hydrological properties regulate grassland ecosystem responses to
1224 multifactor global change: A modeling analysis, *J. Geophys. Res.-Biogeo.*, 113, G03003,
1225 doi:10.1029/2007JG000539, 2008.
- 1226 Wesely, M. L. and Hart, R. L.: Variability of short term eddy-correlation estimates of mass
1227 exchange, in: *The ForestAtmosphere Interaction*, edited by: Hutchinson, B. A., Hicks, B.
1228 B., and Reidel, D., 591-612, Dordrecht, 1985.
- 1229 Wu, J., Kutzbach, L., Jager, D., Wille, C., and Wilmking, M.: Evapotranspiration dynamics in a
1230 boreal peatland and its impact on the water and energy balance, *J. Geophys. Res.-Biogeo.*,
1231 115, G04038, doi:10.1029/2009JG001075, 2010.
- 1232 Zhang, Y., Li, C., Trettin, C. C., Li, H., and Sun, G.: An integrated model of soil, hydrology, and
1233 vegetation for carbon dynamics in wetland ecosystems, *Global Biogeochem. Cy.*, 16, 9-1-
1234 9-17, doi:10.1029/2001GB001838, 2002.

1235 **Figure captions**

1236 **Fig. 1.** Layout for *ecosys* model run to represent biological, chemical and hydrological
1237 characteristics of a Western Canadian fen peatland. Figure is not drawn to scale. D_{hummm} = depth
1238 to the bottom of a layer from the hummock surface; D_{holl} = depth to the bottom of a layer from
1239 the hollow surface; TOC = total organic C (Flanagan and Syed, 2011); TN = total nitrogen
1240 (Flanagan and Syed, 2011); TP = total phosphorus (Flanagan and Syed, 2011); CEC = Cation
1241 exchange capacity (Rippy and Nelson, 2007); the value for pH was obtained from Syed et al.
1242 (2006); WTD_x = external reference water table depth representing average water table depth of
1243 the adjacent ecosystem; L_t = distance from modelled grid cells to the adjacent watershed over
1244 which lateral discharge / recharge occurs

1245 **Fig. 2. (a, c, e, g, i, k)** 3-day moving averages of modelled and EC-gap filled net ecosystem
1246 productivity (NEP) (Flanagan and Syed, 2011), and **(b, d, f, h, j, l)** hourly modelled and half
1247 hourly measured water table depth (WTD) (Syed et al., 2006; Cai et al., 2010; Long et al., 2010;
1248 Flanagan and Syed, 2011) from 2004-2009 at a Western Canadian fen peatland. A positive NEP
1249 means the ecosystem is a carbon sink and a negative NEP means the ecosystem is a carbon
1250 source. A negative WTD represents a depth below hummock/hollow surface and a positive WTD
1251 represents a depth above hummock/hollow surface

1252 **Fig. 3.** Half hourly measured **(a)** incoming shortwave radiation, and **(b)** air temperature (T_a); and
1253 **(c)** hourly modelled and half hourly measured water table depth (WTD) (Syed et al., 2006; Cai et
1254 al.; 2010, Long et al.; 2010, Flanagan and Syed, 2011) during August 2005, 2006 and 2008 at a
1255 Western Canadian fen peatland. A negative WTD represents a depth below hummock/hollow



1256 surface and a positive WTD represents a depth above hummock/hollow surface. Grey arrows
1257 indicate nights with similar temperatures

1258 **Fig. 4. (a)** Half hourly EC-gap filled (Flanagan and Syed, 2011) and hourly modelled ecosystem
1259 net CO₂ fluxes, **(b)** half hourly automated chamber measured (Cai et al., 2010) and hourly
1260 modelled understorey and soil CO₂ fluxes, and **(c)** hourly modelled soil CO₂ and O₂ fluxes
1261 during August 2005, 2006 and 2008 at a Western Canadian fen peatland. A negative flux
1262 represents an upward flux or a flux out of the ecosystem and a positive flux represents a
1263 downward flux or a flux into the ecosystem. Grey arrows indicate nights with similar
1264 temperatures (Fig. 3)

1265 **Fig. 5. (a-c)** Half hourly observed air temperature (T_a), **(d-f)** hourly modelled and half hourly
1266 observed water table depth (WTD) (Syed et al., 2006; Cai et al., 2010; Long et al., 2010;
1267 Flanagan and Syed, 2011), **(g-i)** half hourly EC-gap filled (Flanagan and Syed, 2011) and hourly
1268 modelled ecosystem net CO₂ fluxes, **(j-l)** half hourly automated chamber measured (Cai et al.,
1269 2010) and hourly modelled understorey and soil CO₂ fluxes during July-August 2005, 2006 and
1270 2008 at a Western Canadian fen peatland. A negative flux represents an upward flux or a flux out
1271 of the ecosystem and a positive flux represents a downward flux or a flux into the ecosystem. A
1272 negative WTD represents a depth below hummock/hollow surface and a positive WTD
1273 represents a depth above hummock/hollow surface

1274 **Fig. 6.** Modelled and EC-derived (Flanagan and Syed, 2011) growing season (May-August)
1275 sums of **(a)** net ecosystem productivity (NEP), **(b)** gross primary productivity (GPP), and **(c)**
1276 ecosystem respiration (R_e) during 2004-2009; **(d)** observed mean growing season air temperature
1277 (T_a) and measured and modelled average growing season water table depth (WTD) during 2004-



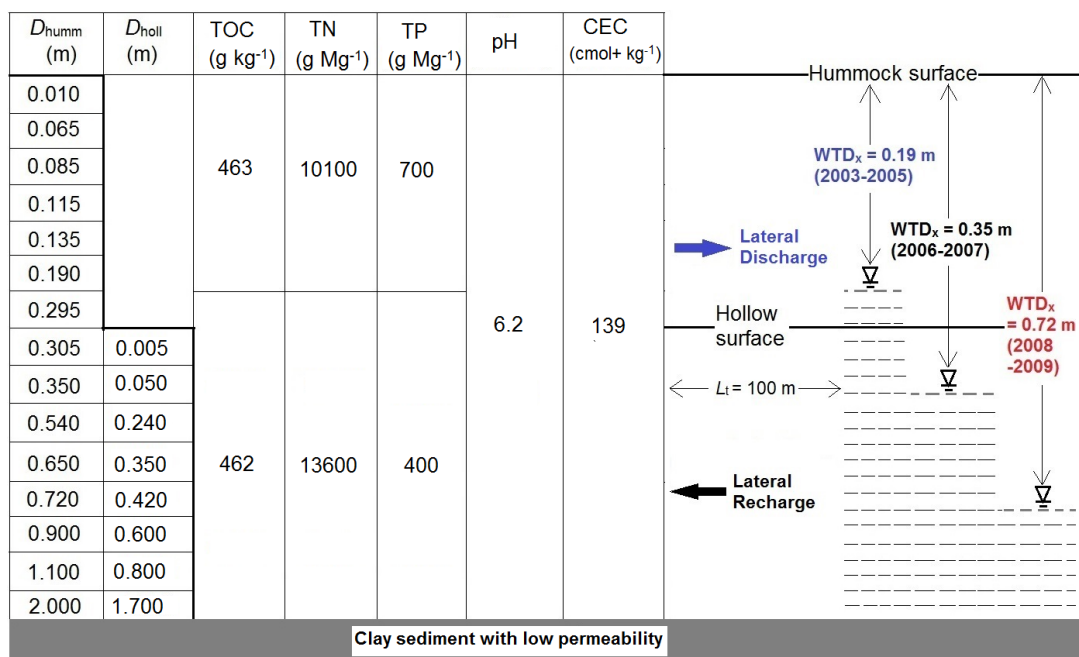
1278 2009; Modelled and EC-derived (Flanagan and Syed, 2011) annual sums of **(e)** NEP, **(f)** GPP,
1279 and **(g)** R_e during 2004-2008; and **(h)** observed mean annual T_a and measured and modelled
1280 average WTD during ice free periods (May-October) of 2004-2008 at a Western Canadian fen
1281 peatland. A negative WTD represents a depth below hollow surface and a positive WTD
1282 represents a depth above hollow surface. A positive NEP means the ecosystem is a carbon sink

1283 **Fig. 7.** Regressions ($P < 0.001$) of growing season (May-August) sums of modelled and EC-
1284 derived (Flanagan and Syed, 2011) **(a)** net ecosystem productivity (NEP), **(b)** gross primary
1285 productivity (GPP), and **(c)** ecosystem respiration (R_e) on growing season averages of modelled
1286 and observed water table depth (WTD) during 2004-2009; and regressions ($P < 0.001$) of annual
1287 sums of modelled and EC-derived (Flanagan and Syed, 2011) **(d)** NEP, **(e)** GPP and **(f)** R_e on
1288 average modelled and measured WTD during ice free periods (May-October) of 2004-2008 at a
1289 Western Canadian fen peatland. A negative WTD represents a depth below hollow surface and a
1290 positive WTD represents a depth above hollow surface. A positive NEP means the ecosystem is
1291 a carbon sink

1292 **Fig. 8.** **(a)** Observed, real-time simulated and projected drainage simulated average growing
1293 season (May-August) water table depth (WTD); EC-derived, real-time simulated and projected
1294 drainage simulated growing season sums of **(b)** net ecosystem productivity (NEP), **(c)** gross
1295 primary productivity (GPP), and **(d)** ecosystem respiration (R_e); and regressions ($P < 0.001$) of
1296 real-time simulated and projected drainage simulated sums of **(e)** NEP, **(f)** GPP, and **(g)** R_e on
1297 real-time simulated and projected drainage simulated average growing season WTD during
1298 2004-2009 at a Western Canadian fen peatland. A negative WTD represents a depth below
1299 hollow surface and a positive WTD represents a depth above hollow surface. A positive NEP
1300 means the ecosystem is a C sink

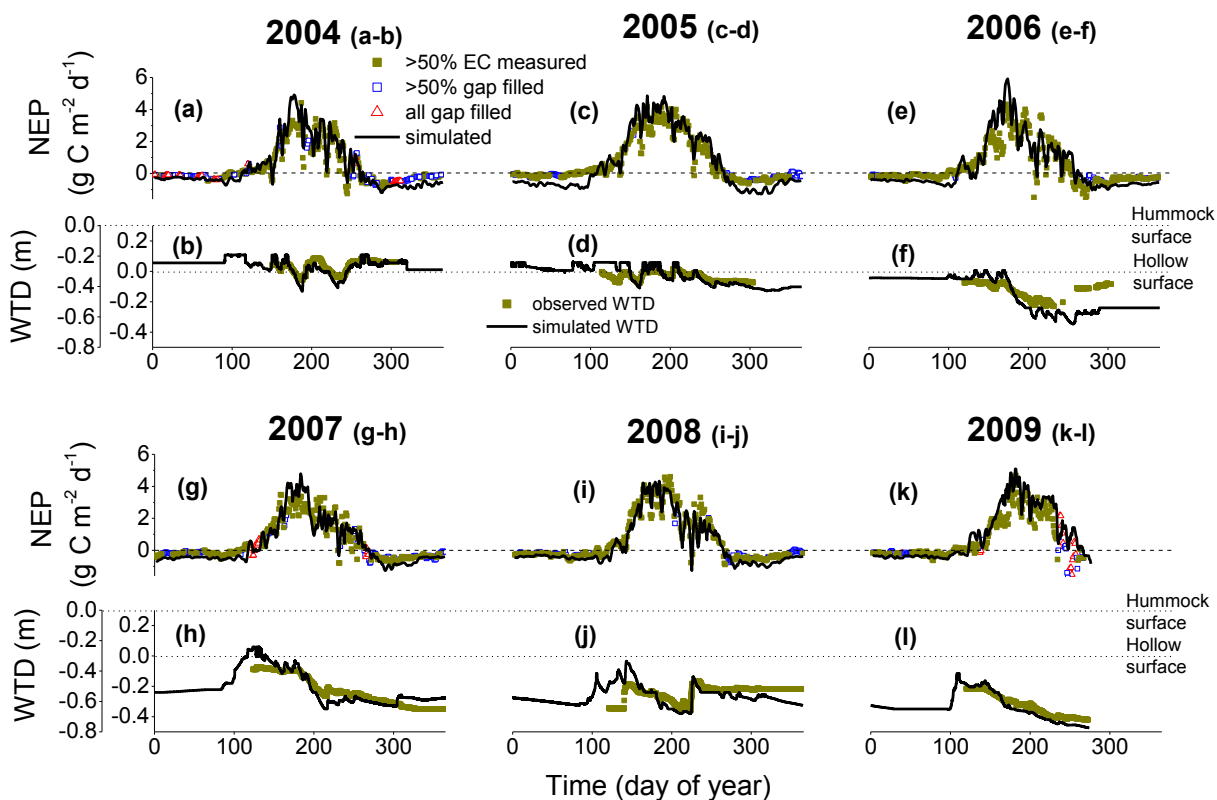


1301 **Fig. 9.** Real-time simulated and projected drainage simulated **(a)** average growing season (May-
1302 August) water table depth (WTD), **(b)** growing season sums of non-vascular (moss) gross
1303 primary productivity (GPP), and **(c)** growing season sums of vascular GPP; and regressions
1304 ($P < 0.001$) of real-time simulated and projected drainage simulated sums of **(d)** non-vascular
1305 GPP, and **(e)** vascular GPP on real-time simulated and projected drainage simulated average
1306 growing season WTD during 2004-2009 at a Western Canadian fen peatland. A negative WTD
1307 represents a depth below hollow surface and a positive WTD represents a depth above hollow
1308 surface



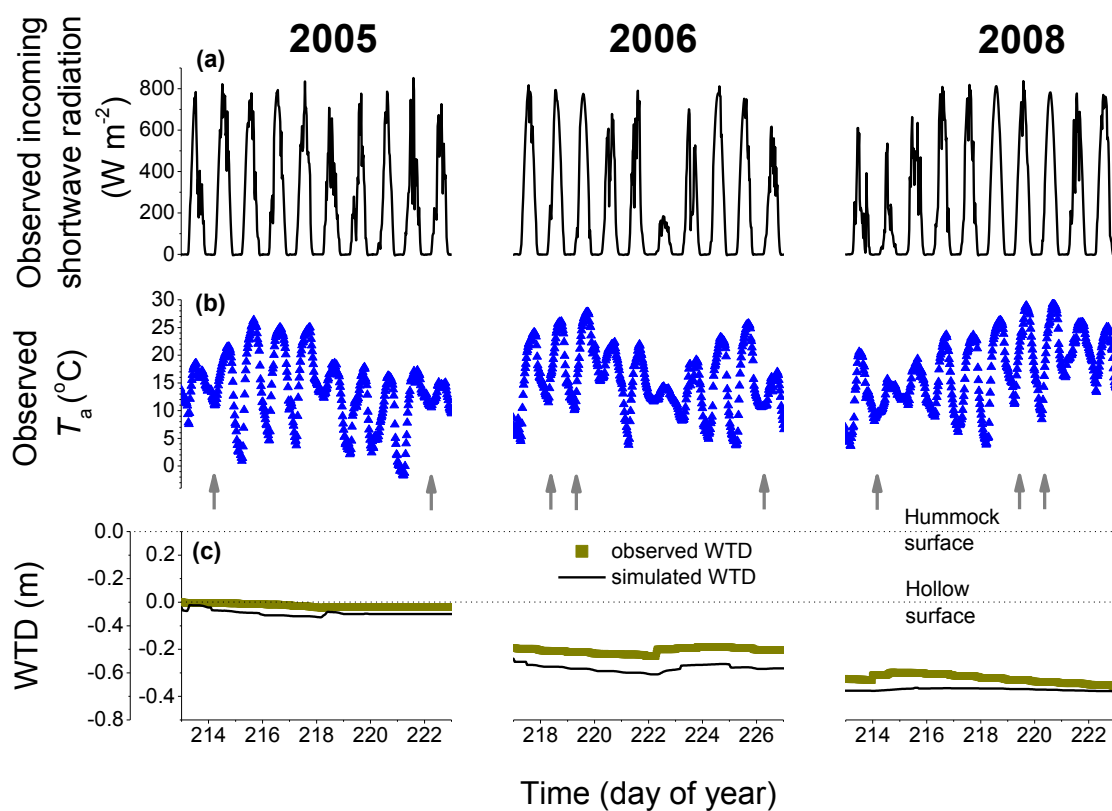
1309

1310 **Fig. 1.**



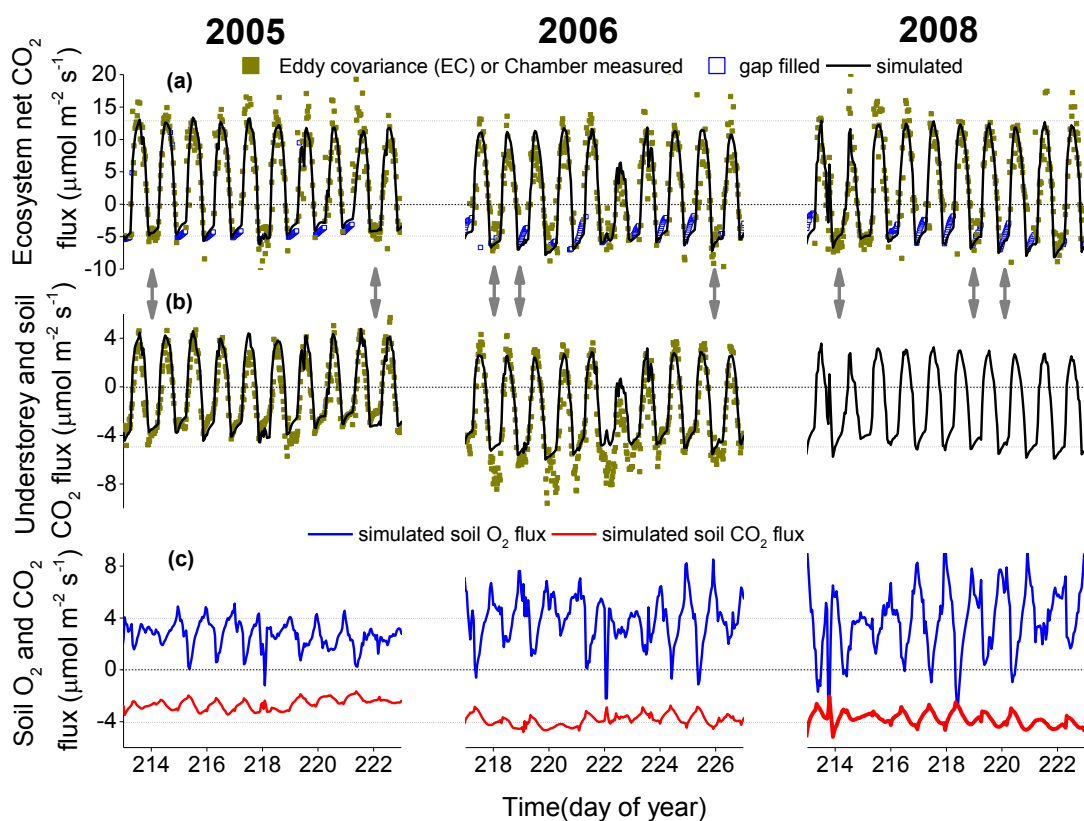
1311

1312 Fig. 2.



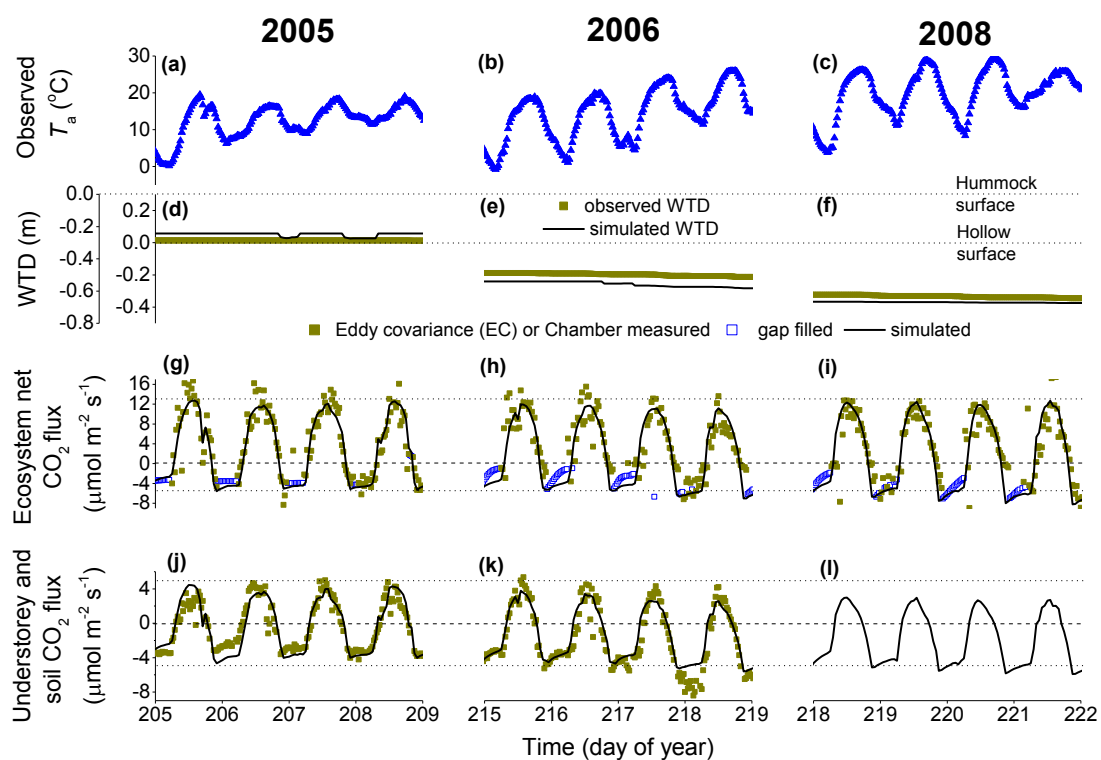
1313

1314 Fig. 3.



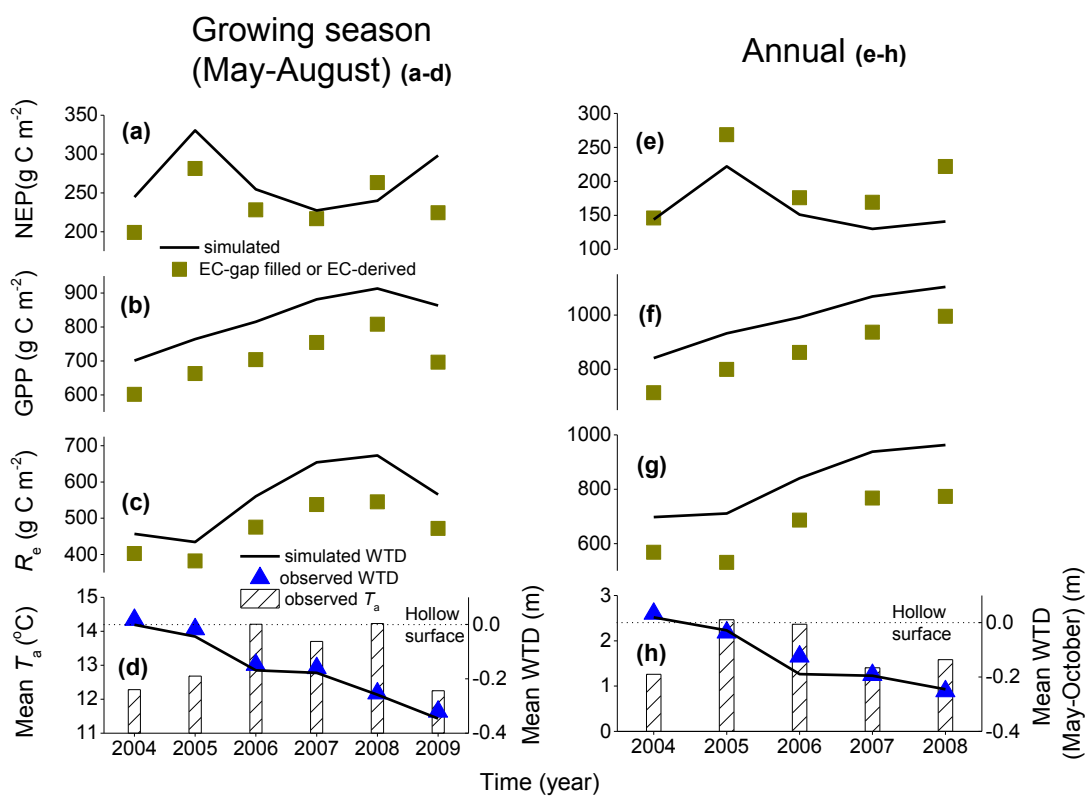
1315

1316 Fig. 4.



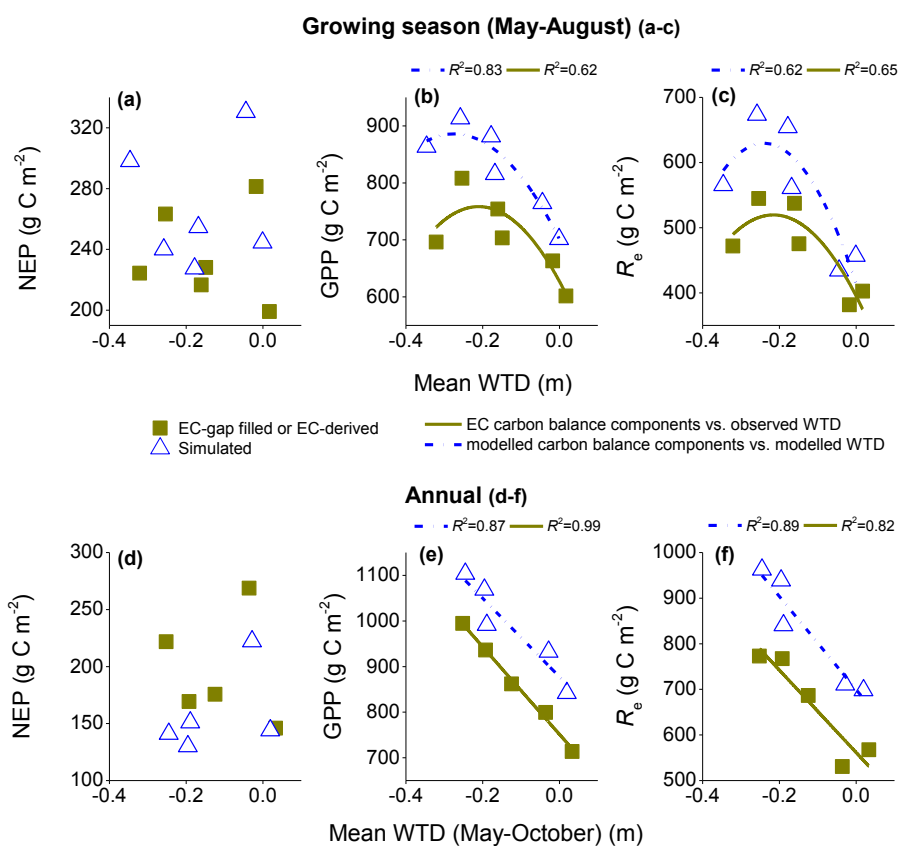
1317

1318 **Fig. 5.**



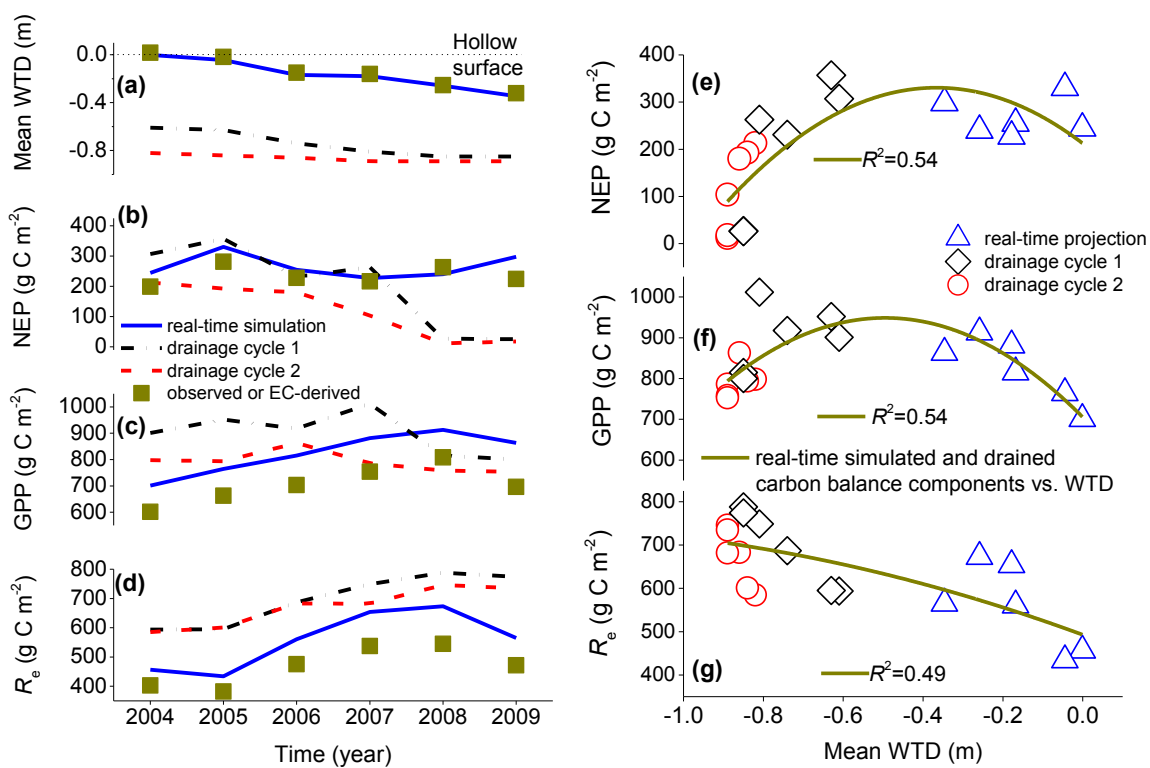
1319

1320 Fig. 6.



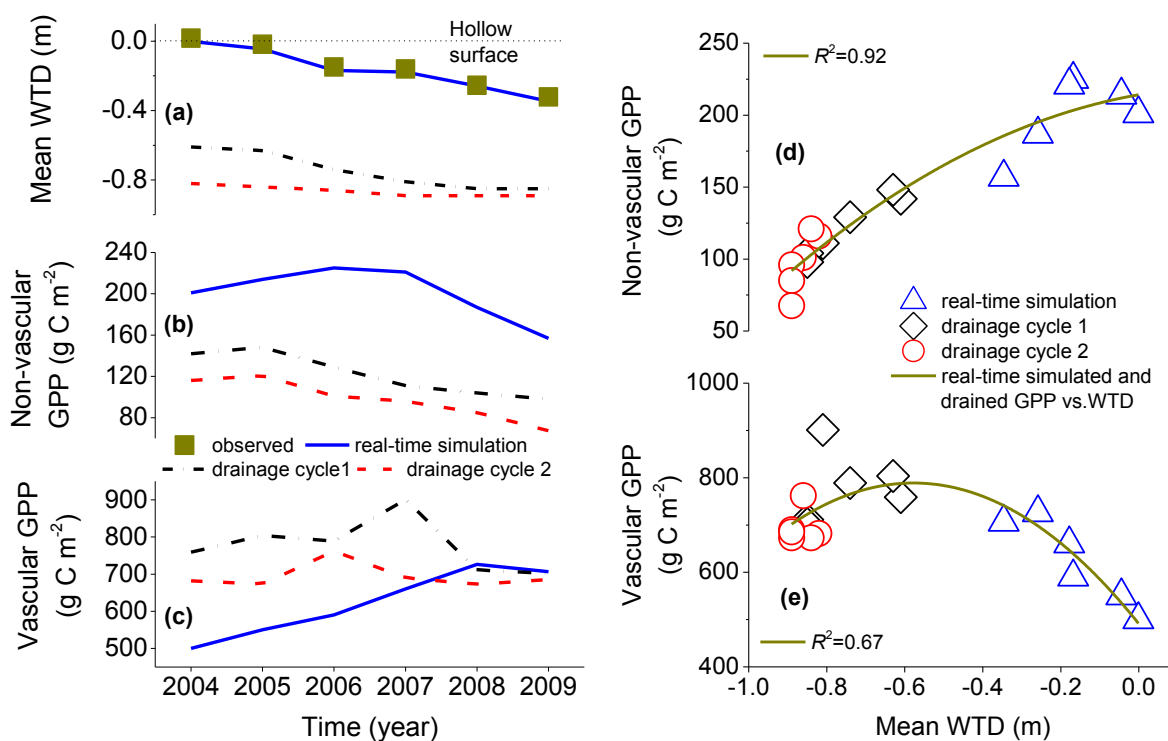
1321

1322 **Fig. 7.**



1323

1324 **Fig. 8.**



1325

1326 **Fig. 9.**



1327 **Table 1:** Statistics from regressions between modelled and EC-gap filled net ecosystem CO₂
 1328 fluxes throughout the years of 2004-2008 at a Western Canadian fen peatland

Year	Total annual precipitation (mm)	<i>n</i>	<i>a</i>	<i>b</i>	<i>R</i> ²	RMSE (μmol m ⁻² s ⁻¹)	RMSRE (μmol m ⁻² s ⁻¹)
Modelled vs. eddy covariance CO ₂ fluxes measured at <i>u</i> * > 0.15 ms ⁻¹							
2004	553	5034	0.08	1.10	0.81	1.58	1.92
2005	387	5953	0.07	1.03	0.82	1.68	1.99
2006	465	6012	0.07	1.08	0.79	1.68	1.98
2007	431	5385	0.06	0.99	0.79	1.83	2.09
2008	494	5843	-0.01	0.98	0.84	1.63	2.02
Modelled vs. gap-filled CO ₂ fluxes							
2004	553	3750	-0.13	1.20	0.89	0.64	
2005	387	2807	-0.49	1.03	0.76	0.82	
2006	465	2748	-0.48	1.15	0.81	0.58	
2007	431	3375	-0.36	0.97	0.74	1.23	
2008	494	2941	-0.54	1.05	0.79	0.95	

1329 (*a*, *b*) from simple linear regressions of modelled on measured. *R*² = coefficient of determination
 1330 and RMSE = root mean square for errors from simple linear regressions of measured on
 1331 simulated. RMSRE = root mean square for random errors in eddy covariance (EC) measurements
 1332 calculated by inputting EC CO₂ fluxes recorded at *u** (friction velocity) > 0.15 m s⁻¹ into
 1333 algorithms for estimation of random errors due to EC CO₂ measurements developed for forests
 1334 by Richardson et al. (2006).



1335 **Table 2:** Statistics from regressions between modelled and EC-gap filled net ecosystem CO₂
 1336 fluxes during the growing seasons of 2004-2009 at a Western Canadian fen peatland

Year	Total growing season precipitation (mm)	<i>n</i>	<i>a</i>	<i>b</i>	<i>R</i> ²	RMSE (μmol m ⁻² s ⁻¹)	RMSRE (μmol m ⁻² s ⁻¹)
Modelled vs. eddy covariance CO ₂ fluxes measured at <i>u</i> * > 0.15 ms ⁻¹							
2004	287	2043	0.55	1.05	0.78	2.27	2.55
2005	276	2200	0.82	0.98	0.79	2.50	2.74
2006	253	2107	0.48	1.06	0.78	2.36	2.76
2007	237	1822	0.65	0.93	0.75	2.91	3.06
2008	276	2070	0.32	0.96	0.82	2.45	2.85
2009	138	1870	0.76	1.01	0.81	2.27	2.83
Modelled vs. gap filled CO ₂ fluxes							
2004	287	837	-0.01	1.21	0.87	1.22	
2005	276	680	-0.57	1.07	0.75	1.26	
2006	253	773	-1.70	0.95	0.73	0.78	
2007	237	1058	-0.51	0.98	0.76	1.88	
2008	276	810	-1.04	1.02	0.79	1.62	
2009	138	1010	-0.02	0.98	0.87	1.20	

1337 (*a*, *b*) from simple linear regressions of modelled on measured. *R*² = coefficient of determination
 1338 and RMSE = root mean square for errors from simple linear regressions of measured on simulated.
 1339 RMSRE = root mean square for random errors in eddy covariance (EC) measurements calculated
 1340 by inputting EC CO₂ fluxes recorded at *u** (friction velocity) > 0.15 m s⁻¹ into algorithms for
 1341 estimation of random errors due to EC CO₂ measurements developed for forests by Richardson et
 1342 al. (2006).